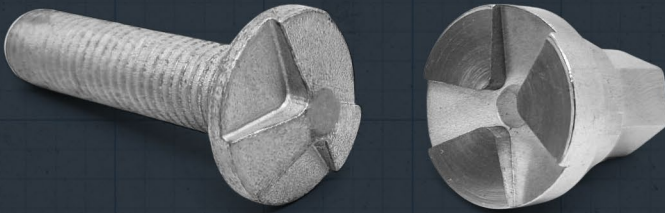


NORM FASTENERS
AR-GE MERKEZİ YAYINLARI
R&D CENTER PUBLICATIONS



— 2023 —

VOLUME 9

NORM
FASTENERS

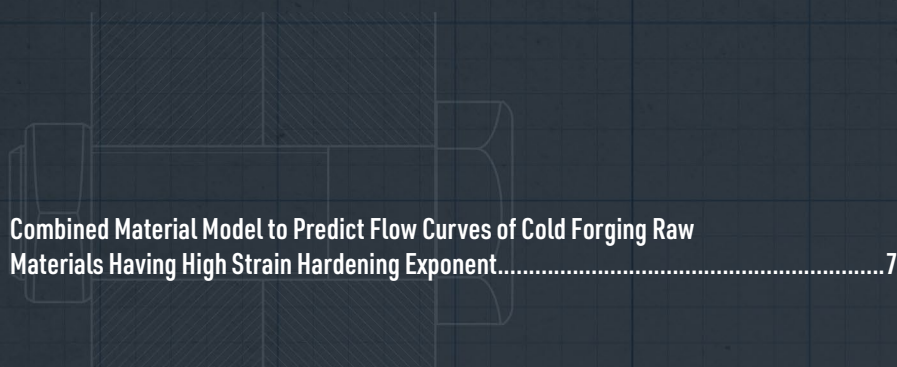
NORM FASTENERS

AR-GE MERKEZİ YAYINLARI

R&D CENTER PUBLICATIONS

Burada yer alan makale ve akademik yazıların tüm hakları yazarlara ve yayınların yapıldığı yayınevlerine ait olup, bu derlemeyi elinde bulunduranlara çoğaltma ve yayma hakkı tanınmaz. Bu hakların ihlali halinde Norm Fasteners'in ve yazarların yasal hakları saklıdır.

All rights to the articles and academic writings contained herein belong to the authors and the respective publisher, and those who hold this compilation do not have the right to reproduce and disseminate the content. In case of infringement of these rights, the legal rights of Norm Fasteners and the authors are reserved.



Combined Material Model to Predict Flow Curves of Cold Forging Raw
Materials Having High Strain Hardening Exponent.....7

Montaj Bölgelerinde Kullanılan Farklı Bağlantı Elemanlarının Düşük Sıkma
Torku Altında Gevşeme Davranışlarının Deneysel Olarak İncelenmesi19

Kamber Ayar Cıvatasının Soğuk Dövme Yöntemiyle Yekpare Üretilmesi.....27

Effect of Cooling Mediums and Process Parameters on Turning of
High-Speed Steels Used in Cold Forging Punches37

A Comparison of Static and Fatigue Performance of High-Strength
Bolts Depending on Heat Treatment Process.....53



Wire-EDM Cutting Strategies of WC-Co Hardmetals: Effect of Number
of EDM Pass on Surface Integrity63



Paslanmaz Çelik Cıvataların Korozyon Dirençlerinin İncelenmesi79

Maximizing Die Life in Cold Forging Dies for Fastener Production:
Parameter Determination and Optimization90

The Investigation of Mechanical Properties and Performance of
Additively Manufactured Stainless Steel Bolts.....92

An Investigation of The Fatigue Life of WC- 26 Wt.% Co Material
Used in Cold Forging Dies94

A Case Study of The Effect of Element Type on The Numerical
Simulation Results of Fastener Cold Forging Production.....96

Investigation of Threading Performance of Self-Threading
Nuts on Machined and Casted Aluminum Parts.....98

ÖN SÖZ

Umut İnce

Norm Fasteners Ar-Ge ve Mühendislik Direktörü

Norm Holding'in sürdürülebilir gelecek vizyonuyla hareket eden bir ekip olarak, her geçen gün Ar-Ge ve inovasyon alanında ivme kazanan yatırımlarımızla sektördeki gelişimi desteklemeye odaklanıyoruz. Değerli iş ortaklarımızla birlikte, geleceğe değer katma misyonumuzu sürdürmek adına kararlı adımlarla ilerliyoruz.

Akademik geçmişe sahip, uzman Ar-Ge ekibimiz ve güçlü iş birliklerimizle birlikte, müşterilerimizin talepleri doğrultusunda katma değeri yüksek çözümler geliştirmenin yanı sıra ulusal ve uluslararası alanda sektöre öncülük eden çalışmalar yürütüyoruz. Her bir projemizde artan motivasyon ve azimle hedeflerimize doğru ilerlerken, teknolojik ilerlemelere katkıda bulunmayı ve sektörümüzde birlikte güçlenerek ilerlemeyi bir sorumluluk olarak görüyoruz.

2023 yılı içerisinde gerçekleştirdiğimiz çalışmaların meyvesini sizlerle paylaşmaktan büyük mutluluk ve gurur duyuyoruz. Bu kitapçık ile birlikte, ortak hedeflerimiz doğrultusunda yürüttüğümüz Ar-Ge faaliyetlerinin sonuçlarını siz değerli iş ortaklarımızla paylaşarak geleceğe değer katmaya devam etmekten memnuniyet duymaktayız.

FOREWORD

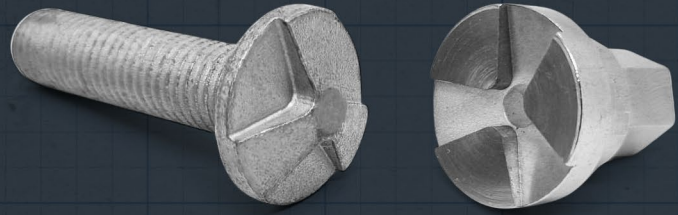
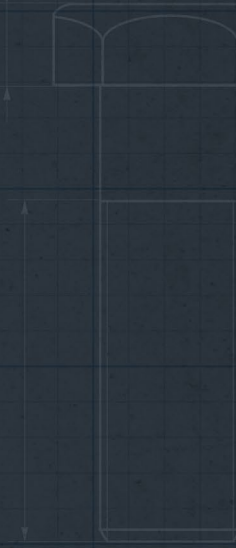
Umut İnce

Norm Fasteners R&D and Engineering Director

Driven by a vision of a sustainable future of Norm Holding, we are a team focused on supporting the development of the sector with our investments gaining momentum in R&D and innovation day by day. Together with our valued business partners, we are moving forward with determined steps to continue our mission of adding value to the future.

With our R&D team of expert researchers with strong academic backgrounds, and strong partnerships, we develop high added value solutions in line with the demands of our customers as well as we conduct pioneering work both nationally and internationally. As we move towards our goals with increasing motivation and determination in each of our project, we see it as a responsibility to contribute to technological advancements and grow stronger together in our industry.

We are thrilled and proud to share with you the fruits of our efforts in 2023. With this booklet, we are pleased to continue adding value to the future by sharing the results of the R&D activities we carry out in line with our common goals with you, our valued business partners.



**COMBINED MATERIAL MODEL
TO PREDICT FLOW CURVES OF
COLD FORGING RAW MATERIALS
HAVING HIGH STRAIN HARDENING
EXPONENT**

*Doğuş ZEREN
Fatih KOCATÜRK
M. Burak TOPARLI*



The 26th International ESAFORM Conference on Material Forming – ESAFORM 2023

COMBINED MATERIAL MODEL TO PREDICT FLOW CURVES OF COLD FORGING RAW MATERIALS HAVING HIGH STRAIN HARDENING EXPONENT

Doğuş ZEREN^{1,a,*}, Fatih KOCATÜRK¹ and M. Burak TOPARLI¹

¹R&D Center, Norm Fasteners

^adogus.zeren@normfasteners.com

Abstract

In order to increase the accuracy of cold forging simulations, flow curves obtained by experimental compression tests are used instead of the material models existing in the software library. The parameters of Ludwik material model were determined with respect to the constructed experimental flow curves at different temperatures and strain rates. Then, the flow curves were defined into the software by using these parameters. While Ludwik model can represent the material flow curve with high accuracy at low plastic strain values, the error rate between the experimental flow curve and the Ludwik model increases at high plastic strain values. Voce material models were known to predict the flow curve of materials with high strain hardening exponents more accurately, especially at high temperature and strain values. In this study, the performance of Ludwik material model was compared to four Voce material models given in the literature and a more accurate combined material model was defined for each flow curve at different temperature and strain rates for 42CrMoS4 material. All experimental flow curves were predicted with a minimum R² of 0.99 and the lowest mean absolute error value with the new combined material model.

Keywords: Metal forming, Voce material model, flow curve prediction, finite element method

1. Introduction

The accuracy of cold forming process simulations using finite element analysis (FEA) software depends on the true stress-plastic strain curves used. In cases where plastic deformation is high, the stress and strain distributions are not uniform, that is, they do not show a certain trend. For this reason, it is difficult to predict the flow curves of steel materials with a high strain hardening exponent, where high plastic strain values are observed in the flow curves, using a single material model. Defining the flow curves of such materials separately according to the deformation transitions increases the accuracy of the prediction models. Plastic deformation transitions in flow curves can be listed as follows: i) the part from the beginning of plastic deformation to the maximum compression stress value, ii) after the maximum compression stress value, the material exhibits strain softening part until the actual rupture of the material. In the literature, there are models such as Hollomon [1], Ludwigson [2], Ludwik [3], Swift [4] and Voce [5] that consider the work hardening rate for material flow curve prediction. However, these models are insufficient to represent the hardening and softening behavior of materials at high plastic strain values. Guo et al. [6] suggested a model that includes both the hardening and softening phases by combining the Voce Model for Hardening [5] and a linear softening model (Voce Model with Linear Softening). The developed model was able to predict the flow stress over a wide plastic strain range. Nguyen [7] has proposed a combination of Voce hardening and Voce softening models. On the other hand, Rotpai et al. [8] proposed a new piecewise model for flow curve prediction at room and elevated temperatures in order to minimize the

deviation between the predicted flow curves and the experimental flow curves. A Swift-Voce model to describe the large deformation behavior of 7050-T7451 aluminum alloy under uniaxial stress, notched stress, and pure shear operations was developed by Cao et al [9]. The combination of Swift model and the 4th order polynomial was also proposed in order to describe the large deformation behavior of the Ti-6Al-4V alloy in the same study. In addition to predicting material flow curves with mathematical models, there are also studies carried out to predict flow curves with machine learning or regression models [10, 11]. An artificial neural network model was suggested by Kocatürk et al. [10] to estimate experimental flow curves of a medium carbon steel material at different temperatures and strain rate values, and the flow curve predictions with high accuracy were obtained with this method. In another study, Aydın et al. [11] proposed a model that can obtain true stress-strain curve from experimental compression test data. Moreover, machine learning models and various regression models were used to predict the flow curves for the intermediate temperature and strain rate values where experimental flow curves are not available and promising flow curves were estimated. In this study, flow curves at different temperatures and strain rates, which were constructed by using the compression test results of a medium carbon alloy steel material, were employed. The parameters of Ludwik Model, Voce Model for Hardening [7], Voce Model for Softening [5], Voce Model with Linear Softening [2] and Voce Model for Hardening and Softening [5] were determined using the "curve_fit" function in the Scipy library on the Python programming language for every temperature and strain rate values. Voce Model for Hardening and Softening best-predicted the flow curve up to maximum compression stress point while Voce model with linear softening and Ludwik Model best-predicted the part from maximum compression stress to the maximum loading point. A new combined material model based on plastic strain subintervals was proposed for the flow curves at different temperatures and strain rates.

2. Materials & Method

The flow curves were obtained from the experimental compression test results of 42CrMoS4 medium carbon alloy steel material. To obtain the flow curves from the experimental compression test data of the materials, the model suggested by Aydın et al. [11] was used. Compression tests were carried out at different temperatures and strain rates in accordance with ASTM E9 standard [12]. Compression tests were performed with a ZWICK universal tensile/compression testing machine for temperatures at 25, 100 and 200°C and strain rates of 0.001 and 0.275 s⁻¹. Before each compression test, MoS₂ based lubricant was used for test plates in order to minimize the friction effects. A model was developed in the Python programming language to compare the performance of the material models used to predict the experimental flow curves obtained. In this model, the material models are defined firstly, then the model coefficients that give the best prediction are determined with the curve fitting method according to the defined plastic strain intervals, and the performances of the models are reported according to the coefficients obtained. The determined coefficients, R² and mean absolute error (MAE) were used for the performance comparison of the obtained flow curves. Functions in the Numpy library were used to calculate the performance criteria. The "curve_fit" function in the Scipy library was used to find the model parameters according to the experimental flow curves. Finally, the Matplotlib library was used to plot the resulting flow curves. The material models used to predict flow curves are defined below. In these models, σ represents the true stress, ϵ the true plastic strain, n is the hardening exponent, and σ_0 , β , K , A , B , C , D , k represent the material coefficients, respectively.

Ludwik model [9]:

$$\sigma = \sigma_0 + K\epsilon^n \quad (1)$$

Voce hardening model [12]:

$$\sigma = \sigma_0(1 - Ae^{-\beta\varepsilon}) \quad (2)$$

Voce softening model [12]:

$$\sigma = \sigma_0(1 - Ae^{\beta\varepsilon}) \quad (3)$$

Voce linear softening model [8]:

$$\sigma = \sigma_0(1 - Ae^{-\beta\varepsilon}) - k\varepsilon \quad (4)$$

Voce hardening and softening model [3]:

$$\sigma = \sigma_0 + A(1 - e^{-B\varepsilon}) + C(1 - e^{D\varepsilon}) \quad (5)$$

3. Comparison of Ludwik and Voce Models

In this section, the flow curve prediction performances of Ludwik and Voce material models in the true plastic strain range of [0, 1.8], which is the whole plastic strain range for 42CrMoS4 material, were compared for 3 different temperatures and 2 different strain rates. The results obtained are given in Table 1. In order to compare the models fairly, the "curve_fit" function in the Scipy library is used with initial parameter values for all models. The Voce Hardening and Softening model best predicted the flow curves at all temperatures and strain rate value of 0.001 s⁻¹ with a minimum R² value of 0.97. For 25 °C and 0.275 s⁻¹ strain rate, the Voce Linear Softening model best predicted the flow curve with 0.97 R², while the Ludwik model best predicted the flow curves at 100 and 200 °C, 0.275 s⁻¹ strain rate with 0.65 and 0.78 R², respectively. Flow curve predictions obtained at 100 °C and strain rate values of 0.001 and 0.275 s⁻¹ were shown in Figure 1 for the plastic strain range of [0, 1.8].

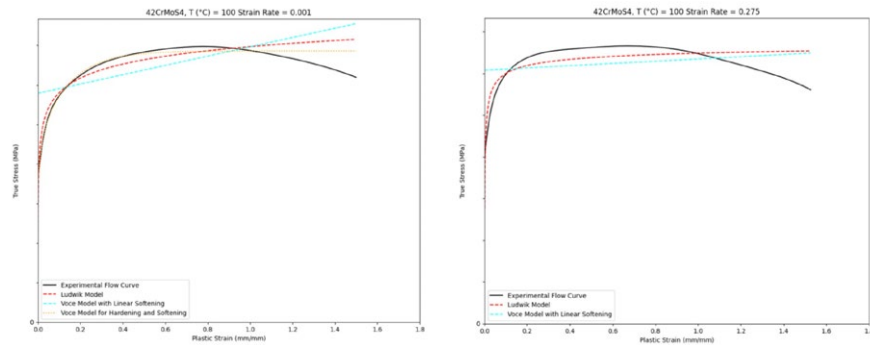


Fig. 1. Flow curve predictions in the plastic strain range of [0, 1.8] for 100 °C, 0.001 and 0.275 s⁻¹ strain rates.

Table 1. Model comparison for plastic strain range of [0, 1.8].

Temperature (°C)	Strain Rate	Model Name	Pl. Str. Inverval	R ²	MAE
25	0.001	Ludwik	0.0-1.8	0.900	1117751
25	0.001	Voce with Linear Softening	0.0-1.8	0.440	2825240
25	0.001	Voce with Hardening and Softening	0.0-1.8	0.980	446045
25	0.275	Ludwik	0.0-1.8	0.600	9942
25	0.275	Voce with Linear Softening	0.0-1.8	0.970	2822
100	0.001	Ludwik	0.0-1.8	0.870	1019870
100	0.001	Voce with Linear Softening	0.0-1.8	0.390	2332653
100	0.001	Voce with Hardening and Softening	0.0-1.8	0.970	438462
100	0.275	Ludwik	0.0-1.8	0.650	7555
100	0.275	Voce with Linear Softening	0.0-1.8	0.050	12002
200	0.001	Ludwik	0.0-1.8	0.880	893179
200	0.001	Voce with Linear Softening	0.0-1.8	0.400	2079574
200	0.001	Voce with Hardening and Softening	0.0-1.8	0.970	370809
200	0.275	Ludwik	0.0-1.8	0.780	6440
200	0.275	Voce with Linear Softening	0.0-1.8	0.190	12061

In order to obtain closer results to the experimental flow curves for 42CrMoS4 material, and to identify models that predict the hardening and softening phases during plastic deformation more accurately, the model predictions for the lower plastic strain ranges were also compared. In order to determine the model that best predicts material behavior up to the maximum compression stress value, the flow curve prediction performances of Ludwik and Voce material models in the true plastic strain range [0, 0.6] were compared for 3 different temperatures and 2 different strain rates. Flow curve predictions obtained at 100 °C and strain rate values of 0.001 and 0.275 s⁻¹ were shown in Figure 2 for the plastic strain range of [0, 0.6]. The results obtained for the true plastic strain range of [0, 0.6] were tabulated in Table 2. The Voce Hardening and Softening model best predicted the flow curves at all temperatures and strain rate values with a minimum R² value of 0.999.

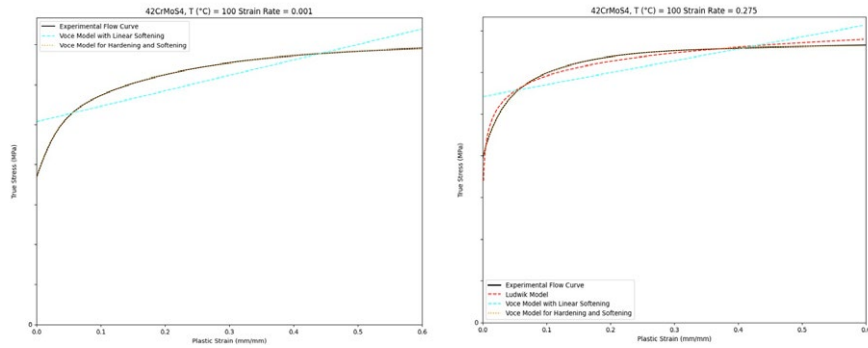


Fig. 2. Flow curve predictions in the plastic strain range of [0, 0.6] for 100 °C, 0.001 and 0.275 s⁻¹ strain rates.

Table 2. Model comparison for plastic strain range of [0, 0.6].

Temperature (°C)	Strain Rate	Model Name	Pl. Str. Interval	R ²	MAE
25	0.001	Voce with Linear Softening	0.0-0.6	0.800	1121473
25	0.001	Voce for Hardening and Softening	0.0-0.6	0.999	9083
25	0.275	Ludwik	0.0-0.6	0.980	1642
25	0.275	Voce with Linear Softening	0.0-0.6	0.660	6054
25	0.275	Voce for Hardening and Softening	0.0-0.6	0.999	86
100	0.001	Voce with Linear Softening	0.0-0.6	0.780	922398
100	0.001	Voce for Hardening and Softening	0.0-0.6	0.999	11076
100	0.275	Ludwik	0.0-0.6	0.970	1474
100	0.275	Voce with Linear Softening	0.0-0.6	0.630	5177
100	0.275	Voce for Hardening and Softening	0.0-0.6	0.999	87
200	0.001	Voce with Linear Softening	0.0-0.6	0.750	849120
200	0.001	Voce for Hardening and Softening	0.0-0.6	0.999	22864
200	0.275	Voce with Linear Softening	0.0-0.6	0.730	4821
200	0.275	Voce for Hardening and Softening	0.0-0.6	0.999	42

In order to determine the model that can predict the hardening and softening behavior of 42CrMoS4 material more accurately, model predictions were compared. For this purpose, the flow curve prediction performances of Ludwik and Voce material models in the plastic strain range of [0.6, 1.8] were compared for three different temperatures and 2 different strain rates. The results were given in Table 3. Flow curve predictions obtained at 100 °C and strain rate values of 0.001 and 0.275 s⁻¹ were shown in Figure 3 for the plastic strain range of [0.6, 1.8]. The Voce Linear Softening model with a minimum R² of 0.78 obtained the best prediction for the flow curves with strain rate of 0.001 s⁻¹ and for all temperature values. The Voce Linear Softening model also obtained the best prediction with 0.92 R² for the flow curve at 200 °C and 0.275 s⁻¹ strain rate. The best predictions for both flow curves at 25 and 100 °C and 0.275 s⁻¹ strain rate were obtained with the Ludwik model with 0.999 R².

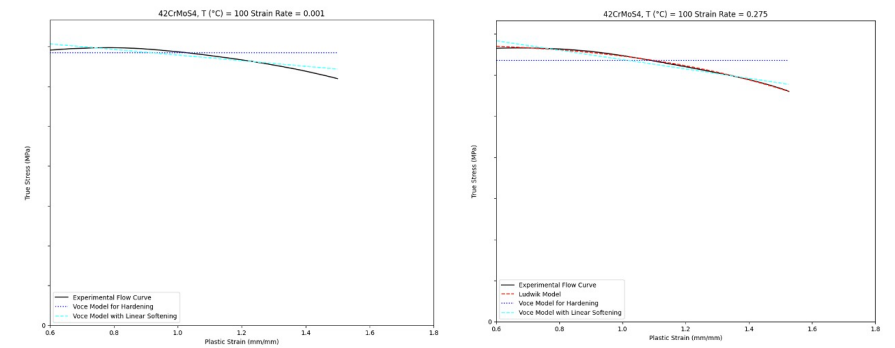


Fig. 3. Flow curve predictions in the plastic strain range of [0.6, 1.8] for 100 °C, 0.001 and 0.275 s⁻¹ strain rates.

Table 3. Model comparison for plastic strain range of [0.6, 1.8].

Temperature (°C)	Strain Rate	Model Name	Pl. Str. Interval	R ²	MAE
25	0.001	Voce with Linear Softening	0.6-1.8	0.850	117884
25	0.275	Ludwik	0.6-1.8	0.999	157
25	0.275	Voce for Hardening	0.6-1.8	0.000	4152
25	0.275	Voce with Linear Softening	0.6-1.8	0.980	617
100	0.001	Voce for Hardening	0.6-1.8	0.000	334923
100	0.001	Voce with Linear Softening	0.6-1.8	0.810	165377
100	0.275	Ludwik	0.6-1.8	0.999	205
100	0.275	Voce for Hardening	0.6-1.8	0.000	3482
100	0.275	Voce with Linear Softening	0.6-1.8	0.930	900
200	0.001	Voce for Hardening	0.6-1.8	0.000	298707
200	0.001	Voce with Linear Softening	0.6-1.8	0.780	159582
200	0.001	Voce for Hardening and Softening	0.6-1.8	0.000	298707
200	0.275	Voce for Hardening	0.6-1.8	0.000	2607
200	0.275	Voce with Linear Softening	0.6-1.8	0.920	734

According to the flow curve prediction results, while the Voce Hardening and Softening model best predicted the material behavior up to the maximum stress point, the Voce Linear Softening and Ludwik models best predicted the hardening and softening behaviors observed after the maximum compression stress value. In order to determine the transition points for these stages, analyzes were carried out to find the model that gives the best estimate in each interval by dividing the whole plastic strain range into 9 equal parts with a true plastic strain range of 0.2. As a result, a new combined material model was determined for each flow curve, which predicts the flow curves very close to the experimental data. The performances of the combined models that give the best predictions at each determined subinterval of true plastic strain range for the flow curves at each temperature and strain rate value were reported in Table 4. Flow curve predictions obtained with the combined model for strain rate values of 0.001 and 0.275 at 100 °C were shown in Figure 4.

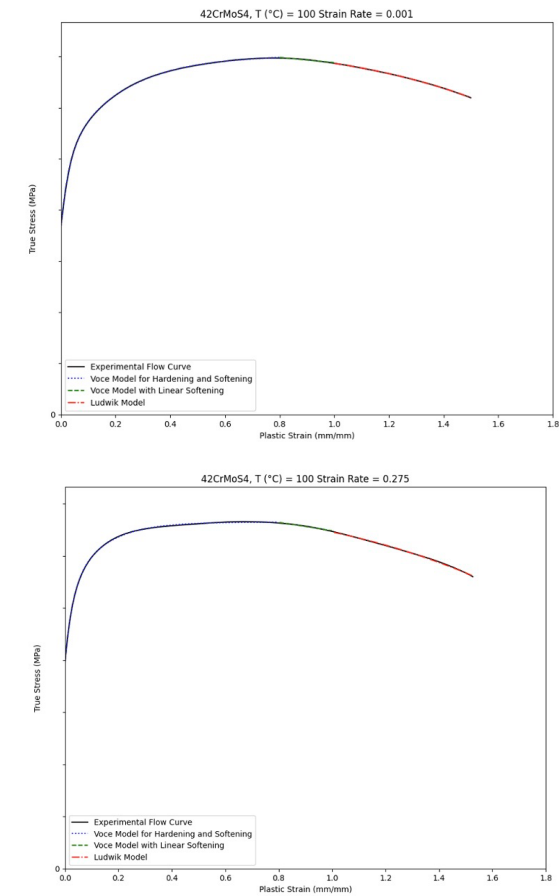
**Fig. 4.** Combined model flow curves of 42CrMoS4 in the plastic strain range of [0, 1.8] for 100 °C, 0.001 and 0.275 s⁻¹ strain rates.

Table 4. Combined model performances for 42CrMoS4 material based on plastic strain range.

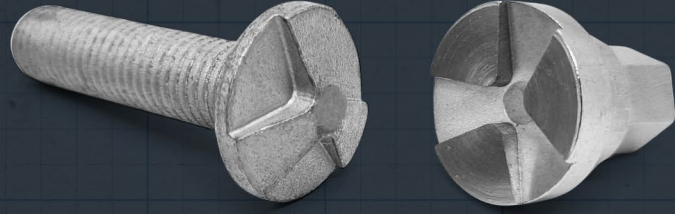
Temperature (°C)	Strain Rate	Model Name	Pl. Str. Inverval	R ²	MAE
25	0.001	Voce for Hardening and Softening	0.0-0.8	0.999	44344
25	0.001	Voce with Linear Softening	0.8-1.0	0.993	1080
25	0.001	Ludwik	1.0-1.8	0.999	709
25	0.275	Voce for Hardening and Softening	0.0-0.6	0.9999	86
25	0.275	Voce with Linear Softening	0.6-1.0	0.968	119
25	0.275	Ludwik	1.0-1.8	0.999	40
100	0.001	Voce for Hardening and Softening	0.0-0.8	0.999	16048
100	0.001	Voce with Linear Softening	0.8-1.0	0.963	3838
100	0.001	Ludwik	1.0-1.8	0.999	830
100	0.275	Voce for Hardening and Softening	0.0-0.8	0.9999	145
100	0.275	Voce with Linear Softening	0.8-1.0	0.981	17
100	0.275	Ludwik	1.0-1.8	0.999	41
200	0.001	Voce for Hardening and Softening	0.0-0.8	0.999	41638
200	0.001	Voce with Linear Softening	0.8-1.0	0.946	4050
200	0.001	Ludwik	1.0-1.8	0.999	1993
200	0.275	Voce for Hardening and Softening	0.0-0.8	0.999	63
200	0.275	Voce with Linear Softening	0.8-1.0	0.987	12
200	0.275	Ludwik	1.0-1.8	0.999	14

Conclusions

Within the scope of the study, flow curves obtained from experimental compression test results of medium carbon alloyed 42CrMoS4 steel were used. The coefficients of both material models were determined for different temperature and strain rate values. In order to fit the curve with model equations, "curve_fit" function in the Scipy library has used on Python programming language. The performances of different material models were also examined by dividing the total plastic strain range into subintervals, and combined piecewise material models were proposed according to the true plastic strain values for each temperature and strain rate value. Flow curve prediction performances of Ludwik material model and four different Voce material models were compared. In the comparisons, the flow curve up to the maximum compression stress point was best predicted by the Voce Hardening and Softening model, while the Ludwik and Voce Linear Softening models best predicted the part after the maximum compression stress point to the breaking point. For the flow curves at different temperatures and strain rates, the new combined material model depending on plastic strain ranges were proposed by using Ludwik and four different Voce models. All experimental flow curves were predicted with a minimum R² of 0.99 and lower absolute error values with the new combined material model while Ludwik model predicted the flow curves with a maximum R² of 0.90.

References

- [1] H. Hollomon, Tensile deformation, Aime Trans. 12 (1945) 1-22.
- [2] D.C. Ludwigson, Modified stress-strain relation for FCC metals and alloys, Metall. Trans. 2 (1971) 2825-2828, <https://doi.org/10.1007/BF02813258>
- [3] P. Ludwik, Elemente der Technologischen Mechanik, Springer, 1909, <https://doi.org/10.1007/978-3-662-40293-1>
- [4] H.W. Swift, Plastic instability under plane stress, J. Mech. Phys. Solids 1 (1952) 1-18, [https://doi.org/10.1016/0022-5096\(52\)90002-1](https://doi.org/10.1016/0022-5096(52)90002-1)
- [5] Voce, The relationship between stress and strain from homogenous deformation, J. Inst. Met. 74 (1948) 537-562.
- [6] J.H. Guo, S.D. Zhao, G.H. Yan, Z.B. Wang, Novel flow stress model of AA 4343 aluminium alloy under high temperature deformation, Mater. Sci. Technol. 29 (2013) 197-203.
- [7] D.T. Nguyen, A new constitutive model for AZ31B magnesium alloy sheet deformed at elevated temperatures and various strain rates, High. Temp. Mater. Process. 33 (2014) 499-508.
- [8] U. Rotpai, T. Arlai, S. Nusen, P. Juijerm, Novel flow stress prediction and work hardening behavior of aluminium alloy AA7075 at room and elevated temperatures, J. Alloy. Compd. 891 (2021) 162013. <https://doi.org/10.1016/j.jallcom.2021.162013>
- [9] J. Cao, F. Li, W. Ma, D. Li, K. Wang, J. Ren, H. Nie, W. Dang, Constitutive equation for describing true stress-strain curves over a large range of strains, Philos. Mag. Lett. 100:10 (2020) 476-485, DOI: 10.1080/09500839.2020.1803508
- [10] F. Kocatürk, M. B. Toparli, B. Tanrikulu, S. Yurttaş, D. Zeren, C. Kılıçaslan, Flow curve prediction of cold forging steel by artificial neural network model, 24th International Conference on Material Forming (2021).
- [11] T. Aydın, F. Kocatürk, D. Zeren, A Model to Construct and Predict Flow Curve of Materials from Compression Test Results with Machine Learning Models Using Python, Key Engineering Materials 926 (2022) 2022-2030, <https://doi.org/10.4028/p-18kwo6>
- [12] ASTM E9-19, Standard Test Methods of Compression Testing of Metallic Materials at Room Temperature, ASTM International, West Conshohocken, PA (2019).



MONTAJ BÖLGELERİNDE KULLANILAN FARKLI BAĞLANTI ELEMANLARININ DÜŞÜK SIKMA TORKU ALTINDA GEVŞEME DAVRANIŞLARININ DENEYSEL OLARAK İNCELENMESİ

*Can İÇMEZ
M. Burak TOPARLI
Umut İNCE*

International Symposium on Automotive Science and Technology - ISASTECH-2023

MONTAJ BÖLGELERİNDE KULLANILAN FARKLI BAĞLANTI ELEMANLARININ DÜŞÜK SIKMA TORKU ALTINDA GEVŞEME DAVRANIŞLARININ DENEYSEL OLARAK İNCELENMESİ

Can İcmez^{1*}, M. Burak Toparlı¹, Umut İnce¹

¹ R&D Center, Norm Cıvata San. ve Tic. A.Ş., AOSB, Çiğli, İzmir, Turkey

*can.icmez@normfasteners.com

Özet

Otomotiv sanayi de dahil olmak üzere bağlantı elemanı kullanılan sektörlerde karşılaşılabilecek en önemli problemlerden bir tanesi gevşemedir. Titreşim testleri (Junker testi), bağlantı elemanlarının gevşeme davranışlarını belirlemek için yaygın olarak kullanılan bir test yöntemidir. Bu test metodu sayesinde farklı cıvata-somun kombinasyonuyla oluşturulan montaj koşullarında gevşeme direncine yönelik testler gerçekleştirilebilmektedir. Titreşim testinin sonucunu etkileyen en önemli parametreler arasında uygulanan tork, kitleme yükü ve sürtünme katsayısı sayılabilir. Bu çalışmada bağlantı elemanlarının düşük sıkma torku altında gevşeme davranışına ilişkin testler gerçekleştirilmiştir. M6x30 DIN933 cıvatalar kullanılarak çift somun, flanşlı somun ve fiberli somun kombinasyonlarıyla farklı montaj koşullarının gevşeme davranışları incelenmiştir. Öncelikle sürtünme katsayılarını hesaplamak için tork-kitleme yükü testleri yapılmıştır. Daha sonra her montaj koşulu için tekrarlı titreşim testleri gerçekleştirilmiştir. Sonuçlar, farklı somun kullanılan montaj koşullarında enine çevrimsel yük altında farklı gevşeme davranışı elde edildiğini göstermektedir. Ayrıca, montaj koşullarında ulaşılan kitleme yükünde sürtünme katsayısının etken olduğu ve titreşim test sonuçlarında önemli bir rol oynadığı görülmüştür. Yapılan testler kapsamında gevşeme direnci en yüksek montaj koşulunun fiberli somun kullanılan seçeneğe olduğu ortaya konmuştur.

Anahtar Kelimeler: Bağlantı elemanı; Cıvata; Gevşeme; Somun; Titreşim testi; Tork.

EXPERIMENTAL INVESTIGATION OF SELF-LOOSENING BEHAVIORS OF DIFFERENT FASTENERS USED IN ASSEMBLIES UNDER LOW TIGHTENING TORQUE

Abstract

Self-loosening is one of the problems that can be observed in industries including automotive in which fasteners are used. Vibration test (Junker test) is one of the widely used testing methods to determine the self-loosening behavior of fasteners. By using this method, self-loosening tests can be conducted on assemblies with different bolt and nut combinations. Some of the important test parameters for vibration tests are applied torque, final clamping load and friction coefficient. In this study, vibration tests on the self-loosening behavior of fasteners under low applied tightening torque were carried out. M6x30 DIN933 bolts with double nut, nut with flange and nut with fiber insert were investigated under transverse cyclic load in order to compare the self-loosening behavior of the assemblies. Firstly, torque-clamp load

tests were done to calculate friction coefficients. After that, repeated vibration tests were conducted for each assembly condition. The results show that assemblies with different nuts behave differently under transverse cyclic load. In addition, the obtained clamping load of each assembly was affected by the friction coefficient, which plays a major role in the vibration tests. According to vibration tests, it was shown that resistance to loosening was highest for the assembly condition with nut with fiber insert.

Keywords: Bolt; Fastener; Nut; Self-loosening; Torque; Vibration test.

1. Giriş

Bağlantı elemanları otomotiv sanayi de dahil olmak üzere endüstrinin bir çok alanında kullanılmaktadır. Karşılaşılan en yaygın sorunların başında bağlantı elemanlarının titreşim altında gevşeme davranışı olduğu söylenebilir. Seçilen cıvata-somun kombinasyonu, ulaşılan kitleme yükü, sürtünme katsayısı, bağlantı yapılan yüzeyin kondüsyonu gibi birçok etken bağlantı elemanlarının gevşeme direncine etki edebilir. Gevşeyen cıvata veya somunlar ani çözümler nedeni ile katastrofik sonuçlar doğurabilir. Bu nedenle bağlantıların sıkma torkları ve ulaşılmak istenen kitleme yükleri bağlantı işleminden önce belirlenmelidir. Titreşim altında gevşeme davranışı gösteren cıvata ve somunları ilk inceleyenlerin başında Junker et al. [1] gelmektedir. Junker'e göre cıvatanın enine yönündeki hareketler gevşeme davranışına neden olmaktadır. Enine titreşim altındaki bağlantı elemanlarının gevşemesi ile ilgili birçok çalışma yapılmıştır. Housari ve Nassar [2] gevşeme davranışı için matematiksel model oluşturup deneysel çalışmalar ile karşılaştırmış ve sürtünme katsayısının gevşemeye etkisini incelemiştir. Sürtünme katsayısının gevşemede çok etkili olduğu sonucuna varmıştır. İnce et al. [3] farklı tipteki somunların gevşeme direncini karşılaştırmıştır. Sanclemente ve Hess [4] gevşeme direncinde etkili olan kitleme yükü, nominal çap ve yüzey sürtünmesi gibi parametreleri karşılaştırarak gevşeme seviyesini ölçen istatistiksel model oluşturmuştur.

Bu çalışmada M6x30 DIN933 cıvatalar ile birlikte çift somun, flanşlı somun ve fiberli somun için 2 Nm tork altında Junker titreşim testleri gerçekleştirilip cıvata somun kombinasyonlarının titreşim altındaki gevşeme davranışları incelenmiştir.

2. Deneysel Test Prosedürü

Bu çalışmada çift somun, flanşlı somun ve fiberli somun olmak üzere toplam üç farklı somun kullanılmıştır. Somunlar ve cıvatalara elektrolitik çinko nikel kaplama işlemi yapılmıştır. Aynı lotta üretilen cıvata ve somunların aynı koşullarda kaplanması ile sürtünme katsayıları da aynı seviyeye getirilmiştir. Testleri yapılan cıvata-somun kombinasyonlarının görselleri Şekil 1'de verilmiştir. Test edilecek numuneler test düzeneğine cıvatanın dönmesi engellenerek somundan sıkılacak şekilde 2 Nm'ye torklanmıştır. Torklanan bağlantı elemanlarının oluşturduğu kitleme yükleri yük sensörü ile ölçülmüştür. Her test kondüsyonu için 10'ar adet olmak üzere toplam 30 tork-kitleme yükü testi ve titreşim testi yapılmıştır. Deneyin ilk bölümünde, her cıvata-somun eşleşmesi için tork-kitleme yükü testleri yapılarak sürtünme katsayıları hesaplanmıştır. Sürtünme katsayıları Denklem (1) ile hesaplanmıştır.

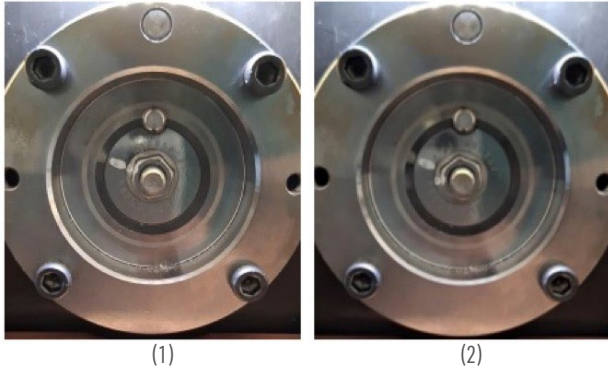


Şekil 1. M6x30 cıvatalar ile çift somun, flanşlı somun ve fiberli somun.

$$\mu_{toplama} = \frac{T/F - P/2\pi}{0.577d_2 + 0.5d_h} \quad (1)$$

burada μ sürtünme katsayısını, T torku, F kitleme yükünü, P diş adımını, d_2 bölüm dairesi çapını ve d_h kafa altındaki efektif çapı belirtmektedir.

Deneylerin ikinci kısmında Junker titreşim testleri yapılmıştır. Testler Vibration Master J160 titreşim cihazında gerçekleştirilmiştir. Bu cihaz Junker testi standardı DIN65151'e [5] uygun olarak Vibration Master firması tarafından üretilmiştir. Test düzeneğine torklanan civata ve somunlar cihaz üzerinde kitleme yükü oluşturmaktadır. Kitleme yükü, yük sensörü ile deney boyunca gerçek zamanlı olarak ölçülmektedir. Test sırasında civataya dik yönde belirli bir mesafe ve frekansta hareket verilmektedir. Tekrarlanan hareket, civata ve somun üzerinde gevşeme davranışına neden olmaktadır (Şekil 2). Civata ve somun gevşedikçe kitleme yükü de azalmaktadır. Titreşim testlerinin genel amacı enine hareket verilen civatanın kitleme yükünün proses boyunca azalma davranışını incelemektir.



Şekil 2. Titreşim testinde gevşemeden öncesi (1) ve sonrası (2) görselleri.

3. Test Sonuçları

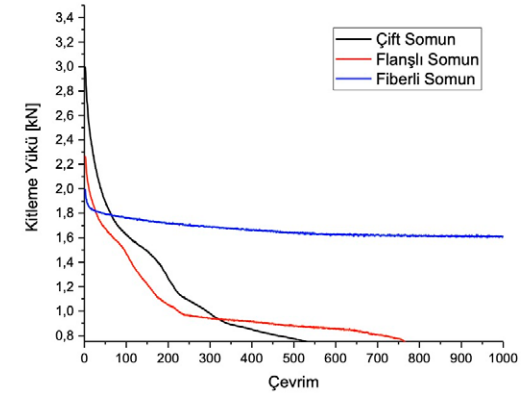
Çift somun ile gerçekleştirilen tork-kitleme yükü testlerinde iki somun da 2 Nm'ye torklanmış olup kitleme yükü ikinci somun torklandıktan sonra ölçülmüştür. Yapılan 10 testin sonucunda ortalama kitleme yükü 2,9 kN ve ortalama sürtünme katsayısı 0,08 olarak hesaplanmıştır.

Flanşlı somun ile gerçekleştirilen tork-kitleme yükü testlerinde flanşlı somun 2 Nm'ye torklanmış olup kitleme yükü somun torklandıktan sonra ölçülmüştür. Yapılan 10 testte ortalama kitleme yükü 2,3 kN ve sürtünme katsayısı 0,11

olarak hesaplanmıştır.

Fiberli somun ile gerçekleştirilen tork-kitleme yükü fiberli somun 2 Nm'ye torklanmış olup kitleme yükü somun torklandıktan sonra ölçülmüştür. Yapılan 10 testte ortalama kitleme yükü 2,0 kN ve sürtünme katsayısı 0,14 olarak hesaplanmıştır. Üç somun arasında sürtünme katsayısı en yüksek olan civata-somun kombinasyonunun fiberli somun kullanılan konfigürasyon olduğu görülmüştür.

Deneylerin ikinci kısmında titreşim testleri yapılmıştır. Çift somun kullanılan konfigürasyonun titreşim testi sonucunda çevrime bağlı olarak kitleme yükündeki azalma eğilimleri incelenmiştir. Çıkan sonuçlara göre, kitleme yükü ilk 100 çevrimde ilk ölçülen yükün yaklaşık %60'ına düşmüştür. Bir civata dışında bütün civatalarda tam gevşeme gerçekleşmiştir. 1000 çevrim sonunda çözülmeyen civatanın kitleme yükü ilk yükünün %30'u seviyesinde ölçülmüştür. Flanşlı somun kullanılan konfigürasyonun gevşeme direnci ölçümleri ile testlere devam edilmiştir. Beş test sonucunda bağlantının 250 çevrime ulaşmadan çözülme görülmüştür. Diğer testlerde yer yer ani düşüşler görülmüş olup genel olarak lineere yakın bir azalma gözlenmiştir. Fiberli somun kullanılan konfigürasyonun titreşim testi sonuçları ile testler sonlandırılmıştır. Yapılan 10 testin hiçbirinde tam gevşeme gerçekleşmemiştir. 1000 çevrimin sonunda civata-fiberli somun üzerinde kalan kitleme yükü ortalama %82 olarak ölçülmüştür. Somun konfigürasyonları için yapılan tüm titreşim testlerinin ortalama sonuçları Şekil 3'te verilmiştir. Elde edilen sonuçlar fiberli somunun diğer iki konfigürasyon ile karşılaştırıldığında daha iyi gevşeme direnci olduğunu göstermektedir. Özellikle uygulanan torkun düşük olması nedeniyle çift somunlu ve flanşlı somun kullanılarak elde edilen testlerde saçılım görece fiberli somunlu konfigürasyona göre daha fazla olduğu ortaya çıkarılmıştır. Fiberli somun kullanılarak elde edilen sonuçlar gevşeme direnci açısından hem daha iyi hem de uygulanan düşük tork miktarına rağmen daha kararlı olarak elde edilmiştir.



Şekil 3. Çift somun, flanşlı somun ve fiberli somunların titreşim altında gevşemelerinin karşılaştırılması.

4. Sonuç

Bu çalışmada çift somun, flanşlı somun ve fiberli somunun titreşim altında gevşeme performansları deneysel olarak incelenmiş ve kitleme yükü kaybına dayalı karşılaştırmalı test sonuçları verilmiştir. Tork-kitleme yükü testleri sürtünme kuvvetlerinin üç kondüsyon için de farklı olduğunu göstermektedir. Sürtünme kuvveti çift somunda ortalama 0,08 hesaplanırken, flanşlı somunda 0,11 ve fiberli somunda 0,14 olarak hesaplanmıştır. Yapılan ölçümlerde 2 Nm'ye torklanan somun civata kombinasyonlarının ilk kitleme yükleri çift somun için 2,9 kN, flanşlı somun için 2,3 kN ve fiberli somun için 2,0 kN olarak ölçülmüştür. Titreşim testlerinde çift somun ve flanşlı somun ile yapılan testlerde fiberli somuna göre çok daha hızlı gevşeme eğilimi görülmüştür. Fiberli somun testlerinde ise tamamen gevşeme görülmemiş olup test sonunda ilk yüklemenin %82'sinin bağlantı üstünde kaldığı görülmüştür. Yürütülen titreşim testleri sonucunda M6 civata ve fiberli somun kombinasyonunun titreşim altında gevşeme direncinin 2 Nm sıkma torkunda çift somun ve flanşlı somuna göre daha yüksek olduğu görülmüştür. Uygulanan düşük tork miktarına rağmen fiberli somun seçeneği daha stabil bir davranış sergilemiştir.

Teşekkür

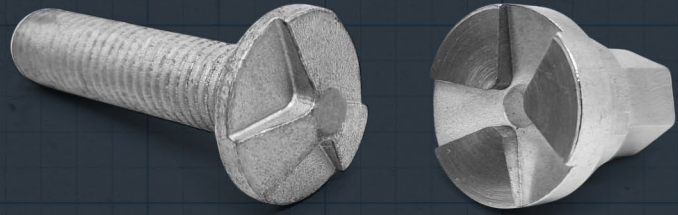
Yazarlar çalışmanın yapılması ve sunulması konusunda sunduğu fırsat için Norm Holding'e teşekkür eder.

Terimlendirme

μ	Sürtünme katsayısı
d_2	Bölüm dairesi çapı (mm)
d_b	Kafa altındaki efektif çap (mm)
F	Kitleme yükü (kN)
kN	Kilo newton
Nm	Newton metre
P	Diş adımı (mm)
T	Tork (Nm)

Kaynaklar

- [1] Junker, G.H., New Criteria for Self-Loosening of Fasteners Under Vibration, SAE Trans. 78 (1969) 314-335. doi:10.4271/690055.
- [2] Housari, B.A., Nassar, S.A., Effect of Thread and Bearing Friction Coefficients on the Vibration-Induced Loosening of Threaded Fasteners, 129 (2007). doi:10.1115/1.2748473.
- [3] İnce, U., Tanrıku, B., Kılıncdemir, E., Yurtdaş, S., Kılıçaslan, C., Experimental investigation on self-loosening of preloaded stainless steel fasteners, Third International Iron & Steel Symposium (2017).
- [4] Sanclemente, J. A., Hess, D. P., Parametric study of threaded fastener loosening due to cyclic transverse loads. Engineering Failure Analysis (2007), 14(1), 239-249. doi:10.1016/j.engfailanal.2005.10.016
- [5] DIN 65151, Aerospace series-dynamic testing of the locking characteristics of fasteners under transverse loading conditions (vibration test) [standard]. Berlin: German Institute for Standardization; 2002.



KAMBER AYAR CIVATASININ SOĞUK DÖVME YÖNTEMİYLE YEKPARE ÜRETİLMESİ

Tolga AYDIN
M. Burak TOPARLI
Umut İNCE



International Symposium on Automotive Science and Technology - ISASTECH-2023

KAMBER AYAR CIVATASININ SOĞUK DÖVME YÖNTEMİYLE YEKPARE ÜRETİLMESİ

Tolga Aydın¹, M. Burak Toparlı¹, Umut İnce¹

¹ R&D Center, Norm Civata San. ve Tic. A.Ş., AOSB, Çiğli, İzmir, Turkey

*tolga.aydin@normfasteners.com

Özet

Araçlarda tekerlekler verilen kamber açısını ayarlamakta kullanılan ekseni kaçık kamber ayar civatalarının yekpare olarak üretilirliği kısıtlıdır. Bunun sebebi, altı köşe kafa bölümünün şaft ile aynı ekseninde olmasına karşın rondela bölümündeki yüksek eksen kaçıklığının soğuk dövme yöntemiyle elde edilmesinin çok zor olmasıdır. Genellikle, ürün soğuk şekillendirme aşamasında ekseni kaçık olan rondela kısmı olmadan üretilmekte ve kafanın altında bulunan altı köşe kademeye rondela çakılarak final ürün formuna ulaşılmaktadır. Ürünün güncel üretim yöntemi kullanıldığında, final ürüne ulaşmak için gereken proses çokluğuyla birlikte yüksek maliyetlere ulaşılmaktadır. Ayrıca, ilave proseslerden dolayı terimler uzamaktadır. Bu çalışmada, kamber ayar civatalarının soğuk dövme yöntemiyle yekpare olarak üretilme kabiliyeti incelenmiştir. Öncelikle ilgili ürünün yekpare üretimi ve ekseni kaçık formların soğuk dövme yöntemiyle üretilmesine yönelik literatür taranmıştır. Nihai ürün formunun eldesi için farklı varyasyonlarda istasyon tasarımları oluşturulmuş ve Simufact Forming sonlu elemanlar programı kullanılarak soğuk dövme prosesinin simülasyonları gerçekleştirilmiştir. Ürün üzerindeki hasar ihtimali, makine tonajı yeterliliği ve istasyon kalıplarındaki gerilmeler gibi kritik tasarım parametreleri kontrol edilmiştir. Sonuç olarak, yapılan tüm çalışmalar üretim denemeleri yapılarak doğrulanmış, kamber ayar civatası yekpare olarak soğuk şekillendirme ile elde edilmiştir.

Anahtar Kelimeler: Kalıp Gerilme Analizi; Kamber Ayar Civatası; Soğuk Dövme; Sonlu Elemanlar Analizi.

MONOLITHIC PRODUCTION OF CAM BOLT VIA COLD FORGING

Abstract

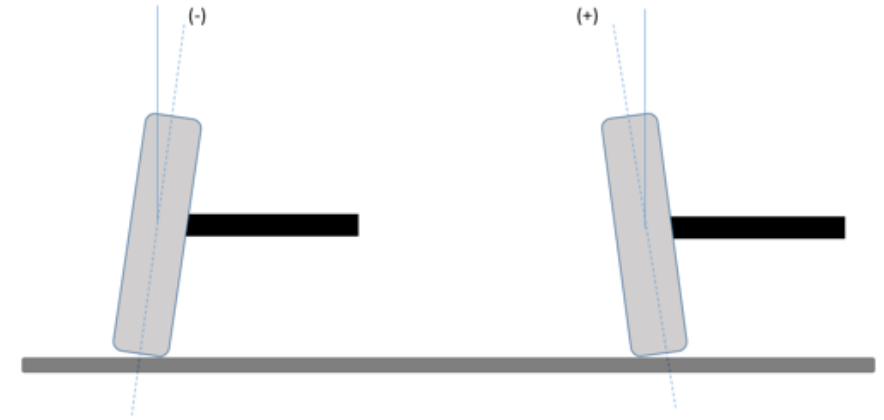
The eccentric cam bolts, which are used to adjust the camber angle given to the wheels in vehicles, have limited manufacturability as one piece. This is because, although the hexagonal head section is coaxial with the shaft, the high eccentricity in the washer section is very challenging to be obtained by the cold forging method. In the current production methodology, the product is cold forged without the eccentric washer section. Then, the final product form is reached by pressing the eccentric washer to the hexagonal section under the head. In the current production method, high costs are reached due to the multi-step processes required to obtain the final product. In addition, lead times are also higher due to the number of additional operations. In this study, the ability of eccentric cam bolts to be produced as a single piece by the cold forging method was investigated. The literature on the monolithic production of cam bolts and the production of eccentric forms by the cold forging method was reviewed. Stage designs in different variations were created and simulations of the cold forging process were carried out using Simufact Forming finite element software. Critical design parameters such as the possibility of ductile damage, the adequacy of the machine tonnage and the stresses on the cold forging dies were investigated. As a result, all the work carried out in this study was verified through production trials

and mono-lithic cam bolt was obtained by using cold forging.

Keywords: Cam Bolt; Cold Forging; Finite Element Analysis; Tool Stress Analysis.

1. Giriş (Introduction)

Otomobillerde, aracın yol ile temasını sağlayan kısmının tekerlekleri olduğu bilinmektedir. Aracın yol tutuşunu artırmak adına yapılan eylemlerden biri ise aracın tekerleklerine kamber açısı vermektir. Kamber açısı, araç lastiklerinin dikey eksene olan açısını belirtmektedir. Pozitif kamber ve negatif kamber olmak üzere Şekil 1'de gösterilmiştir ve genellikle arka tekerlekler verilen 1-2 derecelik negatif kamber açısının viraj performansı açısından tercih edildiği bilinmektedir.



Şekil 1. Pozitif ve negatif kamber açısı.



Şekil 2. Kamber civatası türleri.

Otomobillerin üretim süreçlerinde bu açının istenen şekilde verilmesi adına, OEM firmaları tarafından, "Kamber Ayar Civatası İng. Cam Bolt" olarak isimlendirilen eksen kaçık bir bağlantı elemanı kullanılmaktadır. Şekil 2'de farklı tiplerdeki kamber ayar civataları verilmiştir. Bu civatalar arasından en yaygın olarak kullanılan formun eksen kaçıklığının rondelayla verildiği versiyon olduğu söylenebilir.

Araç tasarımlarına göre, rondelanın çapının ve eksen kaçıklığının değişkenlik göstermesine karşın tasarımların büyük bir çoğunluğu civatanın konvansiyonel tekniklerle soğuk dövülmesini mümkün kılmamaktadır. Civatanın final formuna kavuşması için kafa altında altı köşe formunda olan bir kademe oluşturulmakta ve yuvası aynı geometride olan rondela özel bir makine yardımıyla soğuk şekillendirme mamülü olan civatayla birleştirilmektedir. Bu yöntemle üretilen bir ürünün kafa altı görseli Şekil 3'te verilmiştir. Makine tedarikinin büyük bir ilk yatırım gerektirmesinin yanında dönemsel olarak rondela tedariki konusunda da sıkıntı yaşanabilmekte ve bu ürün gamının üretiminde dışa bağımlı kalınabilmektedir. Satın alınan bu rondelaların, üstündeki ayar işaretleri başta olmak üzere, tolerans dışı temin edilme riski bulunmaktadır. Soğuk şekillendirilen parça üzerinde rondelanın çakıldığı altıköşe kadememin oluşumunda kullanılan sıvama bıçağının düşük çevrimlerde kırıldığı da bilinmektedir [1]. Rondela kalınlığının kademe boyuyla dar bir tolerans içinde uyumlu olması gerekliliği üretim prosesini daha zorlu hale getirmektedir. Tüm bu kalemler toplandığında, üretim bandındaki verimlilik kaybının yanında, proses maliyetleri de yüksek değerlere varabilmektedir. Ek olarak belirli otomotiv firmalarının bu civataları yekpare olarak temin etme isteği, kamber ayar civatalarının yekpare olarak soğuk dövülmesine yönelik yapılan çalışmanın motivasyonunu oluşturmuştur.



Şekil 3. Çakma prosesiyle üretilmiş kamber civatası numunesi.

Soğuk dövmeyle üretim yöntemi, diğer konvansiyonel üretim yöntemleriyle kıyaslandığında; üretim hızı, dar toleranslarda çalışma kabiliyeti, ön ısıtma benzeri ek enerji gereksinimine ihtiyaç duymaması gibi noktalarda avantajlı konumdadır. Avantajlarına karşın soğuk dövme yönteminin, ürün şekillendirilebilirliği ve kullanılan kalıp çevrimleri göz edilerek farklı tasarım parametreleri bulunmaktadır. Özel ürün formlarına olan talep, otomotiv endüstrisindeki gelişmelere paralel olarak, gün geçtikçe artmaktadır. Özel ürün gruplarında soğuk dövülebilirliği araştırma konusunu olan ürün gruplarından biri eksen kaçık ürünlerdir. Ürünlerin üretilebilirliğinin yanında, üretim sürecindeki istasyon tasarımının yorulma

ömrüne de etkisi olduğu konusunda yapılan çalışmalar bulunmaktadır [2]. Proje kapsamında seçilen kamber ayar civatası formunun soğuk şekillendirme ile elde edilmesine dair akademik çalışmaların kısıtlı olmasına karşın Uzakdoğulu araştırmacılar tarafından yapılmış çalışma örnekleri bulunmaktadır. Kim ve diğerleri (2013) kamber ayar civatasının soğuk şekillendirme prosesini sonlu elemanlar programı kullanarak modelleyerek ürün üzerindeki sıcaklık dağılımının değişimini incelemiştir [3]. Cho ve diğerleri (2007) ise aynı formdaki civataların soğuk şekillendirilmesi üzerine çalışma yürütmüştür [4].

Kamber ayar civatasının soğuk dövme yöntemiyle yekpare olarak üretilmesi için çalışılacak forma referans olması adına, elektrikli otomobil üreticilerinden birinin kullandığı, yüksek eksen kaçıklığına ve yüksek rondela çapına sahip bir ürün seçilmiştir. Bahsi geçen formdaki ürünlerin soğuk dövülmesine dair literatür taraması yapıp elde edilen bilgi birikimi kullanılarak seçilen ürün için istasyon tasarımı oluşturulmuştur. Çalışmalar yapılırken; rondela bölgesindeki sünek hasar oluşumu, firma bünyesindeki pres tonajının yeterliliği, kalıp üretim imkanları, kalıp sistemleri ve istasyon tasarımının istasyonlar arası transfer için uygunluğu gibi tasarım parametreleri göz önünde bulundurularak üretim bandında karşılaşılabilecek olası problemlerin minimize edilmesi hedeflenmiştir. Ürün için oluşturulan istasyon kalıpları üç boyutlu modellenerek Simufact Forming programına aktarılmıştır. İstasyon tasarımı ve gerçek üretim koşullarında kullanılan kalıp sistemlerine uygun olarak proses simülasyonu tamamlanıp, simülasyonda final ürüne istenen tasarım parametrelerinde ulaşmak adına ara istasyonlarda tekrarlı olarak şekillenme simülasyonları yapıp optimum kalıp formları tespit edilmiştir. Şekillenme üzerindeki kusurların ve kritik istasyon kalıplarında oluşan yüklerin sonlu elemanlar programı üzerindeki tespitinin ardından üretim denemelerine geçilerek oluşturulan tasarımın denenmesi hedeflenmiştir.

2. Ana Bölüm (Main Section)

Bu bölümde, M14 ovalama ve 38 mm rondela çapına sahip bir kamber ayar civatası seçilmiş, bu ürünün yekpare olarak üretilmesi için yapılan tasarımsal çalışma adımları anlatılmıştır. Ürün, rondela yarıçap değerinin yaklaşık üçte biri oranında eksen kaçıklığına sahip olması ve ürünün kaçıklığının görece yüksek olarak değerlendirilmesi sebebiyle tercih edilmiştir. Ele alınan ürün formu Şekil 4'te verilmiştir.



Şekil 4. Belirlenen civata formu.

Ürün tasarımı yapılırken, ürünün üretim bandındaki şekillenme performansını ve montaj koşullarındaki uygunluğunu etkileyebilecek kritik tasarım parametrelerine dikkat edilmiştir. Bu parametreler, ürünün eksen kaçıklığı ve rondela çapının büyüklüğü dikkate alındığında; flanş kısmında oluşabilecek hasar (çatlak) ihtimalinin incelenmesi, ürünün üretilmesi için gereken toplam tonajın kullanılan yatay pres kapasiteleri içerisinde olması ve kalıpların statik dayanım sınırları içerisinde yer almasıydı. Çatlak oluşumunun önüne geçmenin en önemli yollarında birinin istasyonlar üzerindeki birim şekil değiştirmeyi minimize edip daha geniş çaptaki (bulk) malzemelerle çalışılması olduğu bilinmektedir. Bu sebeple, yüksek

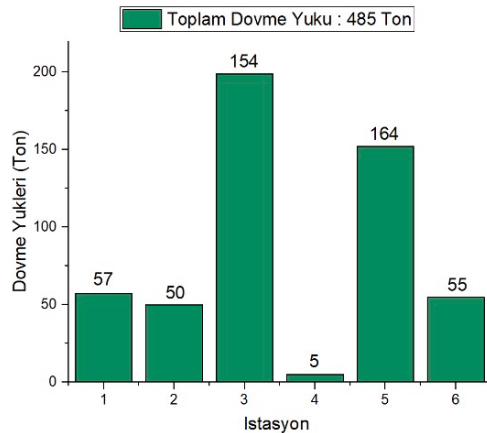
ekstrüzyon oranı kullanarak hem malzemenin rondela kısmındaki olası çatlak ihtimalinin düşürülmesi hem de iş parçasının az pekleştirilerek gerekli tonaj değerine ve kalıp dayanımlarına olumlu etki sağlaması hedeflenmiştir. Birim şekil değiştirmeyi minimize ederken kullanılan yöntemlerden diğeri de armudi istasyonundan başlayarak kafa bölgesindeki kütlelin eksenini kaydırarak malzeme akışını optimize etmek olmuştur. Tonajın istenen maksimum sınırdaki tutulması için ise kalıp sistem ve geometrilerine yönelik çalışmalar iteratif olarak yapılmış, şekillenme uygunluklarına dikkat edilerek finalize edilmiştir.

İncelenen ürün formu için, literatürde bulunan, kafa şişirme prosesi kullanılarak final ürün formu elde edilen üretim stratejisi tercih edilmemiştir. Sebep olarak ise, ürün hazırlık formunun istenildiği gibi şekillenmemesi ve ufak toleranslarda transfer parmakları arasında iş parçasının kayması durumunda oluşabilecek çapak gibi şekillenme kusurlarıdır. Bununla birlikte, şişirilen iş parçasında oluşabilecek çatlak ihtimali de, kafadaki malzemenin görece az olmasından dolayı artacaktır. Bu görüşün ışığında, sıvama prosesinin kullanıldığı bir öncül istasyon tasarımı oluşturulmuştur.

2.1. Simülasyon Çalışmaları

Oluşturulan tasarımlar doğrultusunda; farklı alternatifler denenerek soğuk şekillendirme açısından en uygun istasyon tasarımları Simufact Forming sonlu elemanlar programı kullanılarak belirlenmiştir. Nihai tasarımda, ilk üç istasyonda hazırlık yapılmış, dördüncü ve beşinci istasyonda kafa formu oluşturulmuştur. Son olarak altıncı istasyonda kesme yapılarak final ürün formuna ulaşılması hedeflenmiştir. Nihai istasyon tasarımı sonucunda kalıplar modellenmiş ve simülasyon çalışmaları tamamlanmıştır. Simülasyon çalışmalarından elde edilen final form Şekil 6'da paylaşılmıştır.

Simülasyon çalışmaları sonucunda, elde edilen yarı mamuller ve final ürün formu üzerinde bir kusur görülmemesine karşın proses için gerekli olan dövme yükünün çalışmada kullanılan dövme makinasının maksimum kapasitesi olan 500 tondan fazla olduğu görülmüştür. Durum, kafa hazırlık istasyonundaki vurucu kalıp formunun iteratif simülasyonlarla optimize edilmesi sonucu iyileştirilmiştir. Revize vurucu formu kullanılarak elde edilen istasyon bazlı tonaj değerleri Şekil 5'te verilmiştir. Ürün rondelasında aksel kaçıklığın yüksek olduğu bölgedeki çatlak oluşma olasılığının incelenmesi için Cockcroft-Latham sünek hasar parametresi kontrol edilmiştir. Denklem (1), iş parçası üzerindeki sünek hasarı Simufact Forming programı ile hesaplamak için kullanılmıştır:

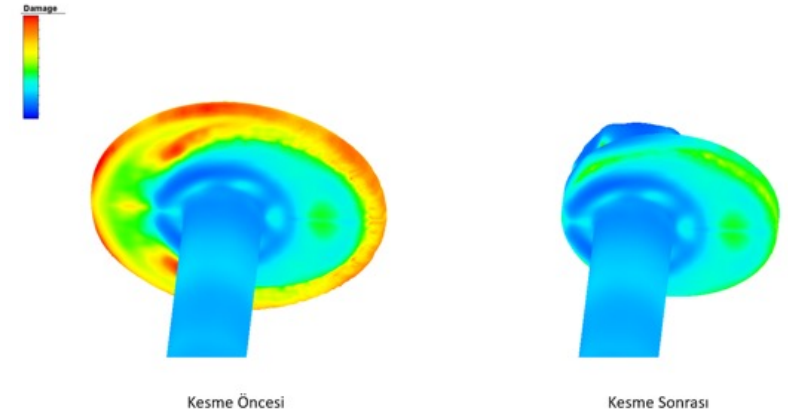


Şekil 5. İstasyon bazlı tonaj değerleri.

$$C \leq \int_0^{\epsilon_f} \sigma_{max} / \sigma_{eff} \epsilon_{eff}^{pl} dt \quad (1)$$

Burada σ_{eff} efektif Von Mises gerilmesini, σ_{max} maksimum asal gerilmeyi, $\epsilon_{eff}^{(pl)}$ efektif plastik gerinim oranını ve ϵ_f hasar durumundaki efektif plastik gerinimi belirtmektedir.

İş parçası üzerinde ölçülen sünek hasar parametresi değerinin kullanılan malzemenin çatlama eşik değerini aşmadığı belirlenmiştir. Final ürün üzerindeki Cockcroft-Latham sünek hasar değeri dağılımı Şekil 6'da verilmiştir.



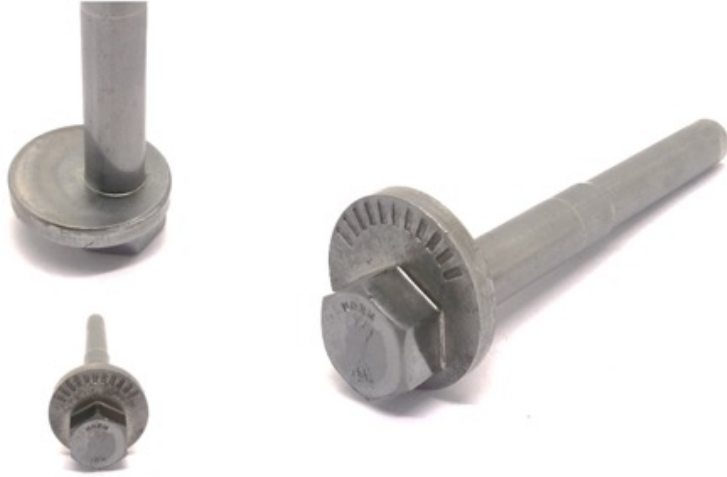
Şekil 6. Simülasyondan alınan Cockcroft-Latham hasar parametresi incelemesi.

Şekillenme açısından ürün formu üzerinde herhangi bir kusur görülmemesi ve soğuk dövme süreci için gereksinim duyulan tonaj değerinin pres kapasiteleri içine girmesi üzerine kritik istasyon kalıpları için kalıp analizi yapılmıştır. İstasyon bazında tonajın en yüksek olduğu kafa hazırlık istasyonunun sabit kalıbı üzerinde oluşan gerilmelerin kullanılan malzemelerin statik dayanım sınırları içerisinde olma durumu incelenmiştir. Kafa hazırlık istasyonu sabit kalıbı malzemesi olarak çekirdek için yüksek kobalt oranı içeren WC-Co, zarf ve kovan malzemesi olarak ise sıcak iş takım çeliği seçilmiştir. Yapılan incelemelerde kalıpların maruz kaldığı yüklerin seçilen malzeme statik dayanım limitleri içinde olduğu ve erken çevrimde kalıp kırılması olmayacağı tespit edilmiştir.

2.2. Üretim Denemeleri

Şekillenme simülasyonlarında herhangi bir hata görülmemesi ve kalıp analizleri sonucunda oluşan değerlerin kalıplarda kullanılan malzemelerin statik dayanım sınırının altında olması sebebiyle üretim denemelerine geçilmiştir. Kalıp tasarımları yapılırken ürünün ağırlık merkezinin alt kısmında olmasına özen gösterilmiştir. Bu sayede, parmaklar arasında iş parçası iletilirken oluşabilecek dönme ihtimali azaltılmıştır. Üretim denemeleri esnasında, tasarım aşamasında dikkat

edilen parametrelerden; tonaj sebebiyle emniyet civatası kopması veya makine arızası veya kafa dövme istasyonunda yüksek kalıp sarfiyatı, rondela bölgesinde hasar oluşumu ve istasyonlar arası iş parçası taşınmasında kayma problemlerinden herhangi biriyle karşılaşmamıştır. Soğuk şekillendirme prosesi sonunda elde edilen final ürün formu Şekil 7'de verilmiştir.



Şekil 7. Soğuk şekillendirilmiş final ürün.

3. Sonuç (Conclusions)

Yapılan çalışmada, otomotiv sektöründe kullanılan kamber ayar civatasının yekpare olarak soğuk şekillendirilebilirliği incelenmiştir. Şekil 4'te verilen ürün formunda kullanılması gereken istasyon tasarımı ve incelenmesi gereken kritik tasarım parametreleri belirlenmiştir. Ürün üzerinde hasar oluşma ihtimali, dövme yüklerinin pres kapasitelerine uygunluğu ve soğuk şekillendirme kalıpları üzerinde oluşan gerilmelerin kontrolü sonlu elemanlar yönteminden faydalanarak yapılmıştır. İteratif simülasyonlar sonucu proses parametreleri optimize edilmiştir. Yapılan tüm çalışmalar sonucunda istasyon tasarımları belirlenmiş ve kalıplar hazırlanmıştır. Üretim denemeleri sonucunda da kamber ayar civatası yekpare olarak soğuk şekillendirme yöntemi ile elde edilmiştir.

Teşekkür (Acknowledgment)

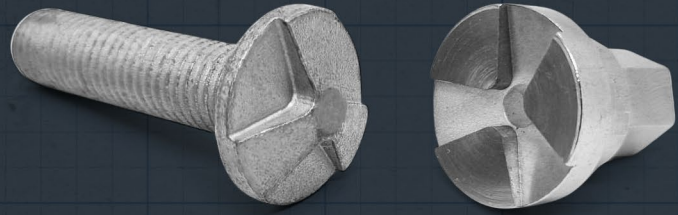
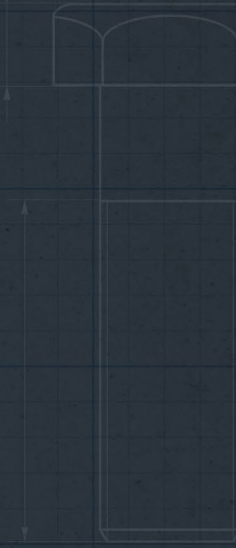
Yazarlar çalışmanın yapılması ve sunulması konusunda sunduğu fırsat için Norm Holding'e teşekkür eder.

Terimlendirme (Nomenclature)

σ_{eff}	Efektif Von Mises Gerilmesi (MPa)
σ_{max}	Maksimum Asal Gerilme (MPa)
$\epsilon_{\text{eff}}^{(p)}$	Efektif Plastik Gerinim Oranı (s-1)
ϵ_f	Hasar Plastik Gerinimi (mm/mm)

Kaynaklar (References)

- Doğan S, Kılıçarslan C, Yurtdaş S, Toparlı M.B. Soğuk Dövme Prosesinde Kullanılan Bir Sivama Kalıbının Sonlu Elemanlar Yöntemi ile İncelenmesi. The 4th International Conference of Materials and Engineering Technology (TICMET'22). September 2022.
- Yurtdaş S, Toparlı M.B, Doğan S, Zeren D, Ince U. Effect of Stage Design on Failure of M16X47 Eccentric Fasteners Used in Automotive Industry. 4. International Conference on Materials Science, Mechanical and Automotive Engineerings and Technology (IMSMATEC'21). May 2021.
- Kim D. B, Kim S, Park J. G, Shin H. S, Kim W. Y, Lee J, Lee I. H, & Cho H. Prediction of temperature distributions of cold forging process for a CamBolt by FEM. Applied Mechanics and Materials. 2013;404: 207-212. <https://doi.org/10.4028/www.scientific.net/AMM.404.207>
- 김완중조해용, 박남기이석진, Cho H. Y, Kim W.J, Lee S.J, Park N.K, Lee, S.H. (n.d.). 서론 1. 비축대칭 캠 볼트 단조의 유한요소 해석 Finite Element Analysis for Forging of Nonaxisymmetric Cam Bolt. 2007.



EFFECT OF COOLING MEDIUMS AND PROCESS PARAMETERS ON TURNING OF HIGH-SPEED STEELS USED IN COLD FORGING PUNCHES

*M. Burak TOPARLI
Sarper DOĞAN
Can İÇMEZ
Umut İNCE*



56th ICFG Plenary Meeting Middle East Technical University (METU) Ankara - Turkey

EFFECT OF COOLING MEDIUMS AND PROCESS PARAMETERS ON TURNING OF HIGH-SPEED STEELS USED IN COLD FORGING PUNCHES

M. Burak Toparlı, Sarper Doğan, Can İçmez, Umut İnce

Norm Fasteners, IAOSB 10007. Sok No: 1/1 Çiğli, İzmir, Türkiye
Corresponding author: M. Burak Toparlı

Abstract

In this study, the influence of cooling mediums namely air, oil and LN₂ during the turning of 1.3343 high-speed steels (HSS) were investigated. Surface roughness of workpieces and flank wear of cutting inserts were compared. The effects of cooling mediums as well as feed rate and cutting length were investigated. Furthermore, SEM investigations and EDS analyses were conducted on workpieces after machining with cryogenic cooling. Residual stress measurements with XRD were also conducted on the samples machined with LN₂. Based on the trials, it was shown that cryogenic cooling excels other coolant mediums in terms of tool wear and surface roughness. Compressive residual stresses along the machining direction were observed for the samples machined with all cooling mediums. There was no recast or white layer observed at the surface of samples machined with all cooling mediums. Therefore, it was concluded that in addition to being environmentally friendly i.e. no requirement for recycling as in oil-based cooling mediums, cryogenic cooling offered advantages in terms of surface integrity of both cutting inserts and machined samples.

Cryogenic cooling, Liquid nitrogen, Turning, High-speed steel, Tool wear, Surface roughness, SEM, Residual stress

1. Introduction

Machinability and tool life are highly influenced by heat generation and thermal conductivity, especially for high-strength steel materials. [1] In order to reduce heat generation and wear on inserts, air and oil cooling methods are widely used. However, air cooling can be insufficient regarding the cooling of inserts and workpieces, particularly for the machining of hard materials. Therefore, premature tool damage can be observed. The oil cooling is not environmentally friendly and may cause health problems on long exposures. The recycling of oil or water-based coolants can be both problematic and costly. Cryogenic cooling, on the other hand, can be a solution to these problems. The air we breathe consists of 79% nitrogen, which makes it naturally recycled after it is used. [2]

In the literature, there are different studies on cryogenic cooling-assisted machining. Potta [3] conducted experiments on 17-4 PH stainless steel comparing air, oil and cryogenic cooling. As a result, thanks to cryogenic cooling, both wear reduction on tools and better surface roughness on workpieces were achieved. Agrawal et al. [4] investigated the machinability of Ti-6Al-4V material with cryogenic cooling and stated that tool life was improved by 200% and 80% relative to dry and wet turning, respectively. In addition, 71% and 64% decrease in surface roughness values relative to dry and wet cooling methods were reported. Ayed et al. [5] measured cutting forces during cryogenic turning for different flow rates and observed an increase in forces concerning flow rate.

The aim of this study is to investigate the influence of cooling mediums namely air, oil and LN₂ during the turning of 1.3343 high-speed steel, used in different areas including cold forging punches. The surface roughness of workpieces and flank wear of cutting inserts with different cutting parameters such as feed rate and cutting length were compared.

Residual stress measurements and SEM investigations coupled with EDS analyses were also conducted to observe the effects of cooling mediums and process parameters.

2. Experimental Procedure

In the experiments, cylindrical workpieces are used. The material for the workpieces was chosen to be 1.3343 high-speed steel (HSS), used in cold forging punches. The chemical composition of 1.3343 steel is given in Table 1. After the trials with different cutting tools, the CBN insert was chosen for the experiments. Rockwell hardness tests were made before the experiments and the hardness of the workpieces was determined to be 60.4 ± 0.5 HRC.

Table 1. Chemical composition of 1.3343 steel workpiece.

	C	Cr	Mo	V	W
1.3343 HSS	0.90	4.1	5.0	1.9	6.4

Before the trials, all of the cutting inserts were photographed (Figure 1) separately. The flank wear values were measured on macroscopic images (Figure 2). Mitutoyo - SJ-210 surface roughness device was used for surface roughness measurements. Residual stress measurements via X-ray Diffraction were conducted by Stresstech X300. After the production trials of 1.3343 hardened steel materials were completed (after the samples were processed 7100 m), residual stresses at the workpiece surfaces were measured to analyse the effect of different cooling mediums and different processing parameters. Measurements were taken at 0° and 90° with respect to machining direction. SEM and EDS analyses were carried out by using FEI Quanta 250 FEG.

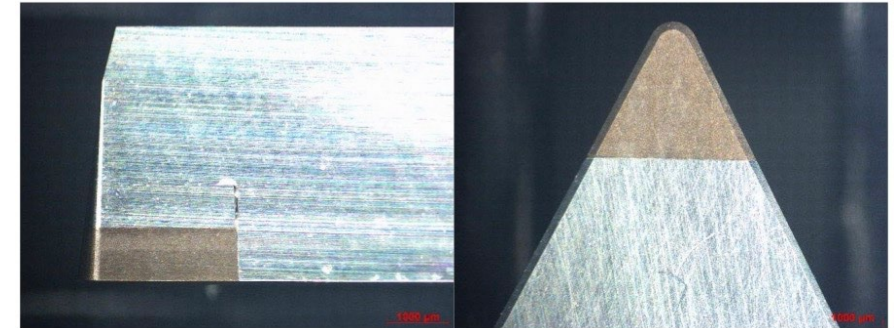


Figure 1. Macroscopic image of CBN insert.

The turning process parameters used in the experiments are given in Table 2. For each parameter set, trials were carried out with 3 different cooling mediums: air, oil and LN₂. The cutting lengths of 1400, 4300 and 7100 m and feed rates of 0.05 and 0.1 mm/rev were determined and related measurements on the cutting tools and machined parts were carried out at these levels. A total of 18 sets of trials were conducted by using 1.3343 high-speed steel samples.

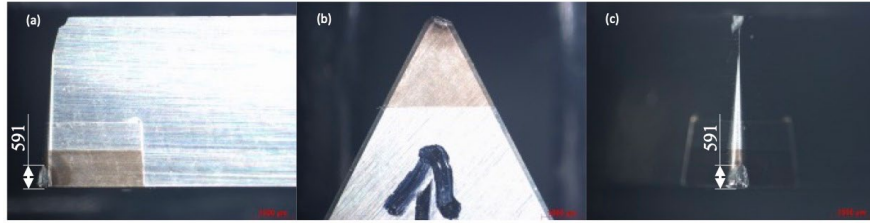


Figure 2. (a) Flank, (b) nose and (c) top view of an insert after cutting operation.

Table 2. Process parameters for turning operations.

	Cooling Medium	Cutting Speed - Vc (m/min)	Feed - f (mm/rev)	Cutting Depth (mm)	Cutting Length (m)
Parameters-1	Air	200	0.05	0.1	1400
Parameters-2	Air	200	0.05	0.1	4300
Parameters-3	Air	200	0.05	0.1	7100
Parameters-4	Air	200	0.1	0.1	1400
Parameters-5	Air	200	0.1	0.1	4300
Parameters-6	Air	200	0.1	0.1	7100
Parameters-7	Oil	200	0.05	0.1	1400
Parameters-8	Oil	200	0.05	0.1	4300
Parameters-9	Oil	200	0.05	0.1	7100
Parameters-10	Oil	200	0.1	0.1	1400
Parameters-11	Oil	200	0.1	0.1	4300
Parameters-12	Oil	200	0.1	0.1	7100
Parameters-13	LN2	200	0.05	0.1	1400
Parameters-14	LN2	200	0.05	0.1	4300
Parameters-15	LN2	200	0.05	0.1	7100
Parameters-16	LN2	200	0.1	0.1	1400
Parameters-17	LN2	200	0.1	0.1	4300
Parameters-18	LN2	200	0.1	0.1	7100

3. Results and Discussions

3.1. Macroscopic Examinations

In Figure 3 (a) and (b), images of cutting tools were given for each parameter set with the corresponding cooling medium as well as feed rates and cutting lengths. After macroscopic examinations of the flank wear, an increase in wear was observed for higher cutting lengths. In terms of insert wear, cryogenic cooling with LN₂ enabled the least tool wear compared to air and oil cooling mediums. In addition, there was no insert failure for cryogenic cooling, however, there were insert tip fractures for air and oil cooling mediums.

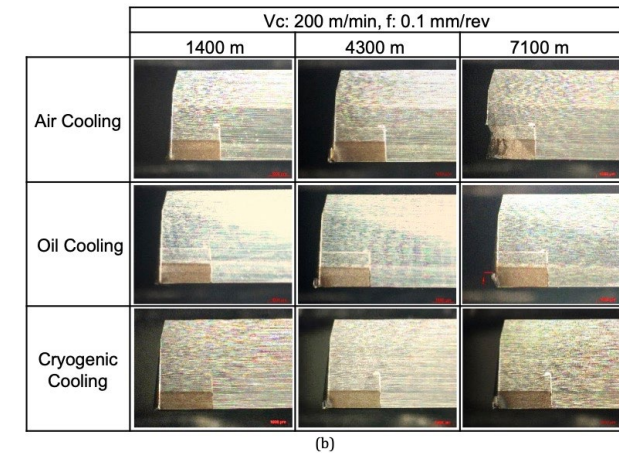
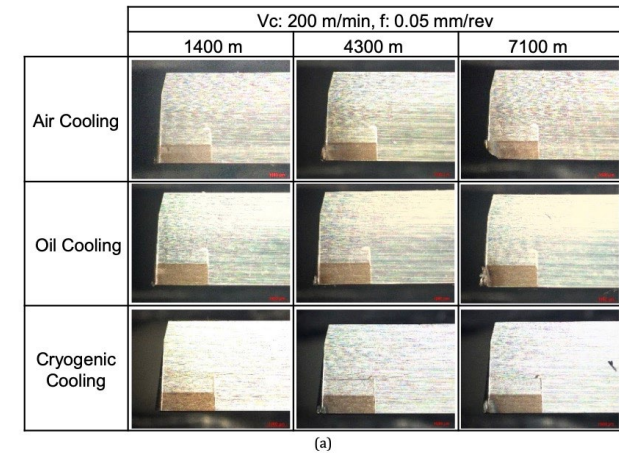


Figure 3. Macroscopic images of inserts for a feed rate of (a) 0.05 and (b) 0.1 mm/rev for all cutting lengths and cooling mediums

3.2. Flank Wear and Surface Roughness

In Figure 4 (a) and (b), the surface roughness R_a and R_z values of the workpieces with a cutting speed of 200 m/min and feed rate of 0.05 mm/rev parameters are given. As can be expected, an increase in cutting length leads to an increase in surface roughness for all cooling mediums. The insert failed after 4300 m cutting length for the air cooling, therefore, the surface roughness values were not reported for that specific condition.

In Figure 4 (c), the comparison of flank wear of the inserts is given. Failure of the cutting insert was observed in air cooling before reaching 7100 m, as stated. The flank wear was the minimum for the cryogenic cooling for all cutting lengths. With oil cooling, no insert failure was observed, however, the flank wear was higher compared to cryogenic cooling, particularly for the cutting length of 7100 m.

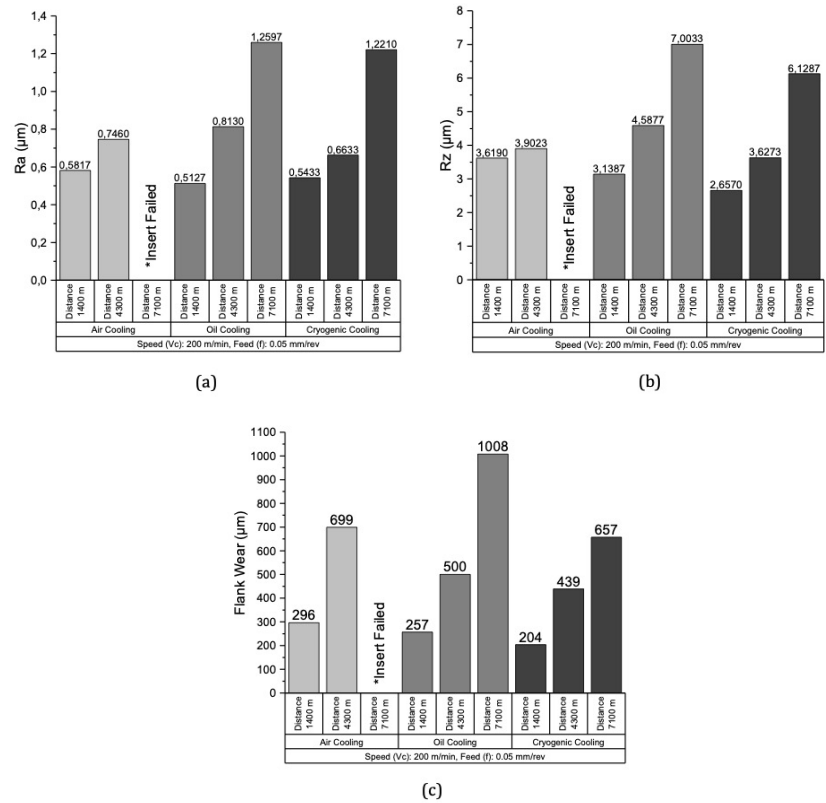


Figure 4. (a) R_a , (b) R_z values of the workpiece and (c) Flank wear of cutting tool with parameters of cutting speed: 200 m/min and feed: 0.05mm/rev

In Figure 5 (a) and (b), the surface roughness R_a and R_z values of the workpieces with a cutting speed of 200 m/min and feed rate of 0.1 mm/rev parameters are given. Compared to trials with a feed rate of 0.05 mm/rev, insert failures were observed for air and oil cooling conditions after the cutting length of 4100 m. As the cutting length is increased, the surface roughness values tend to increase, as can be expected. The surface roughness values were lower for cryogenic cooling. In Figure 5 (c), the comparison of flank wear of the inserts is given. Failures of the cutting tools were observed in air and oil cooling conditions before reaching 7100 m, as stated. The flank wear was the minimum for the LN₂ cryogenic cooling for all cutting lengths.

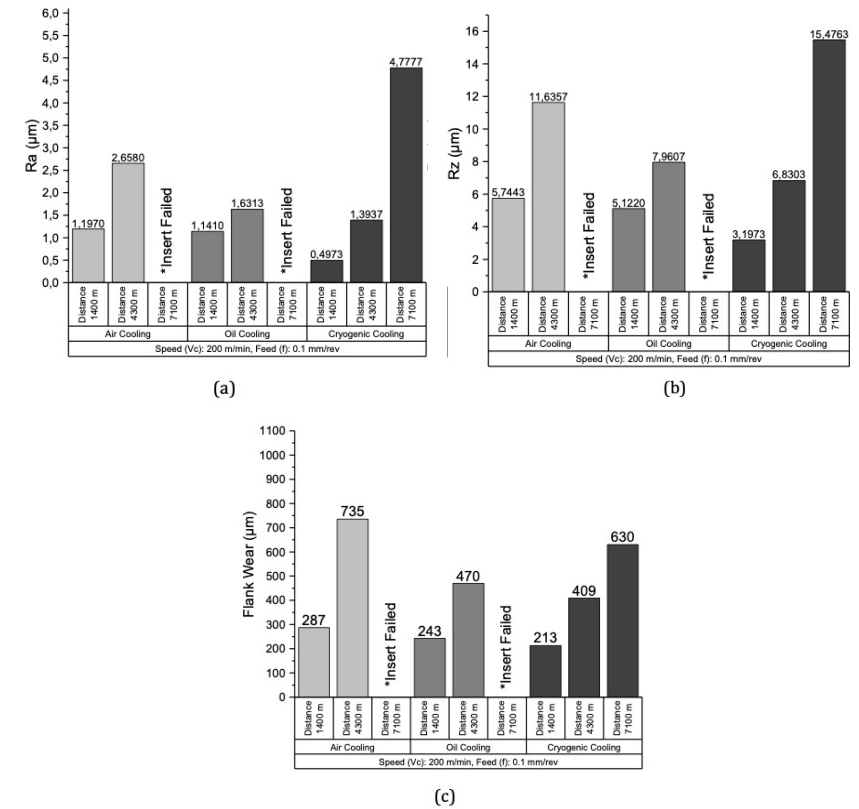


Figure 5. (a) R_a , (b) R_z values of the workpiece and (c) Flank wear of cutting tool with parameters of cutting speed: 200 m/min and feed: 0.1mm/rev

In Figure 6 (a) and (b), the effect of feed rate on the surface roughness values of the workpieces machined with cryogenic cooling is given. The surface roughness values obtained with 0.1 mm/rev were higher for the cutting length of 4300 m and 7100 m. However, R_a and R_z values were similar at 1400 m. In Figure 6 (c), the flank wear of the inserts was compared for the feed rates of 0.05 mm/rev and 0.1 mm/rev. The wear observed for both conditions under cryogenic cooling was similar to each other.

As shown in the surface roughness measurements and flank wear comparisons, cryogenic cooling offered both better surface roughness values and lower insert wear compared to air and oil cooling mediums. This can lead to a decrease in unit cost per part and increase productivity. Considering the trials with 0.1 mm/rev feed rate, an increase in productivity can be achieved by decreasing the cycle time per part for the turning operation of a specific application. Having said that, the surface roughness values tend to increase with higher feed rate. Therefore, depending on the expectations from the turning operation process parameters can be chosen accordingly.

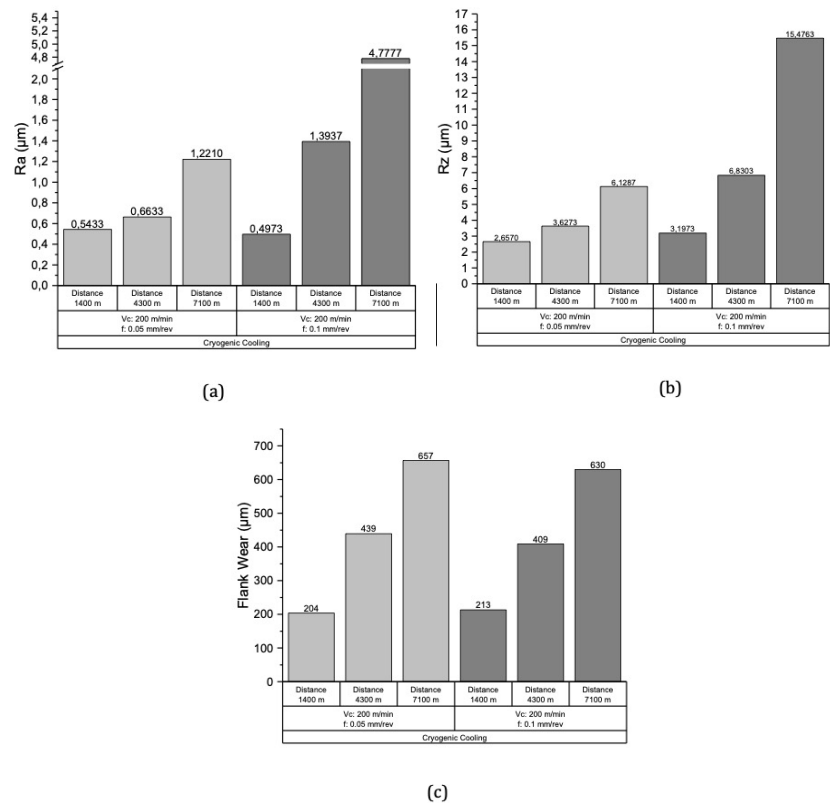


Figure 6. (a) R_a , (b) R_z values of the workpiece and (c) Flank wear of cutting tools that use the cryogenic cooling method.

3.3. Residual Stress Measurements

In Figure 7 (a), residual stress fields after turning with different cooling mediums of 1.3343 steel are given at 200 m/min cutting speed, 0.1 mm/rev feed rate and 0.1 mm depth of cut. Depending on the direction, the residual stress fields changed significantly from compressive to tensile. In the direction of machining labeled as 0° , the residual stresses were compressive and the maximum compressive residual stresses were obtained for oil cooling. As given in Figure 7 (b), when the feed rate was 0.05 mm/rev, the residual stress fields become more compressive reaching -800 MPa with very close to zero residual stresses perpendicular to the machining direction, i.e. 90° , for cryogenic cooling. Therefore, it was shown that decrease in feed rate from 0.1 to 0.05 mm/rev induces more compressive residual stresses at the machined part surface which enables higher fatigue performance by delaying or inhibiting crack initiation and propagation.

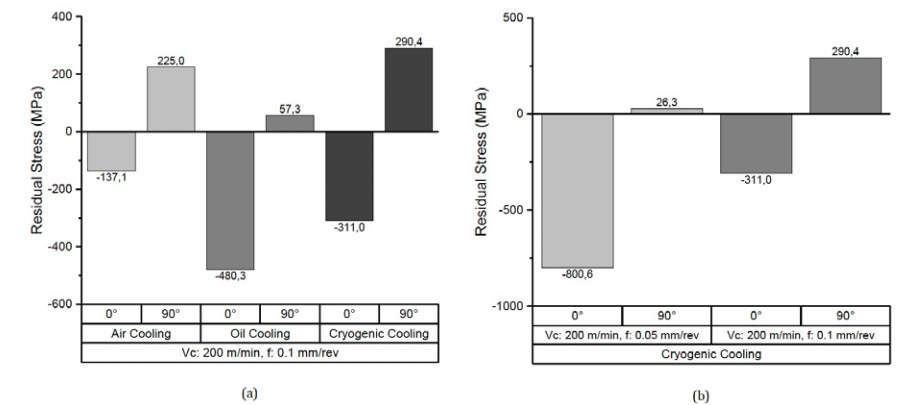


Figure 7. Residual stress measurement (a) different coolant effect, (b) different parameter effect.

3.4. SEM and EDS Analyses

After the turning trials were completed, SEM images were obtained from the surfaces of workpieces for detailed investigations. In particular, SEM images and EDS studies were carried out for the inspection of recast or white layer formation. First, the surfaces were examined before turning, which are given in Figure 8. Main alloying elements including W, Cr, V and Mo were seen in the microstructure, which was shown by EDS analyses (Figure 9).

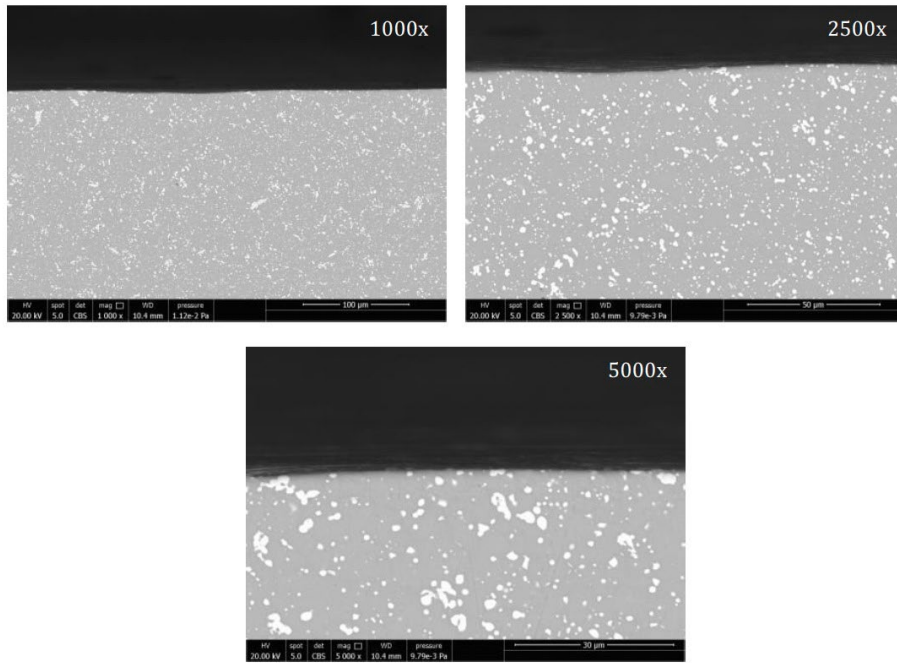


Figure 8. SEM images of 1.3343 steel with different magnifications.

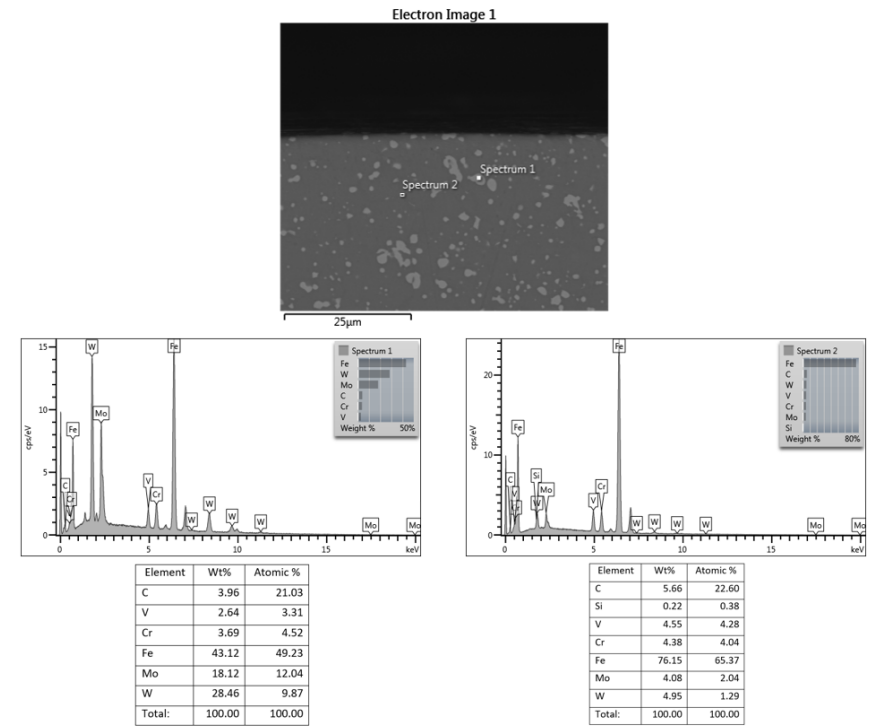


Figure 9. EDS analysis of 1.3343 steel.

Within the scope of SEM investigations, the samples were examined in detail after 7100 m of cutting length at cutting speed of 200 m/min, feed rate of 0.1 mm/rev and cutting depth of 0.1 mm. In the examinations, no recast layer, white layer or any other structure was found after air, oil and cryogenic cooling (Figure 10).

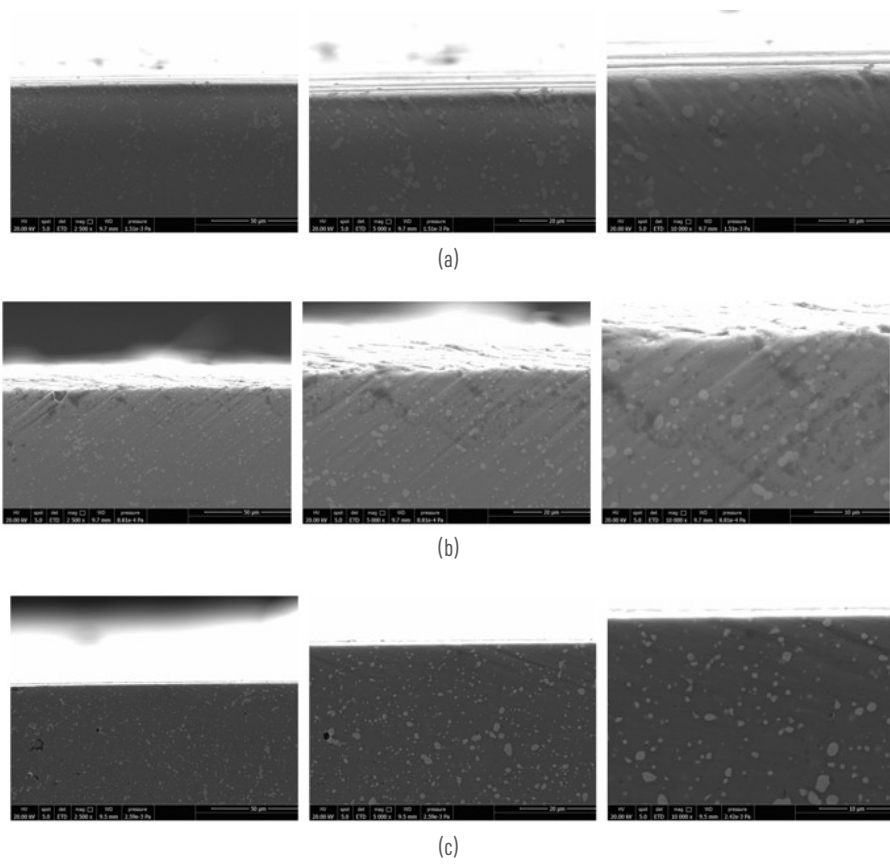


Figure 10. SEM images on different magnifications for (a) air cooling, (b) oil cooling and (c) cryogenic cooling methods.

Investigations related to the recast layer and white layer were detailed with EDS analyses. No significant composition difference between the surface and the base material was found in all cooling mediums (Figure 11). Therefore, it was revealed that no traces of recast or white layer was found by using SEM images and EDS analyses.

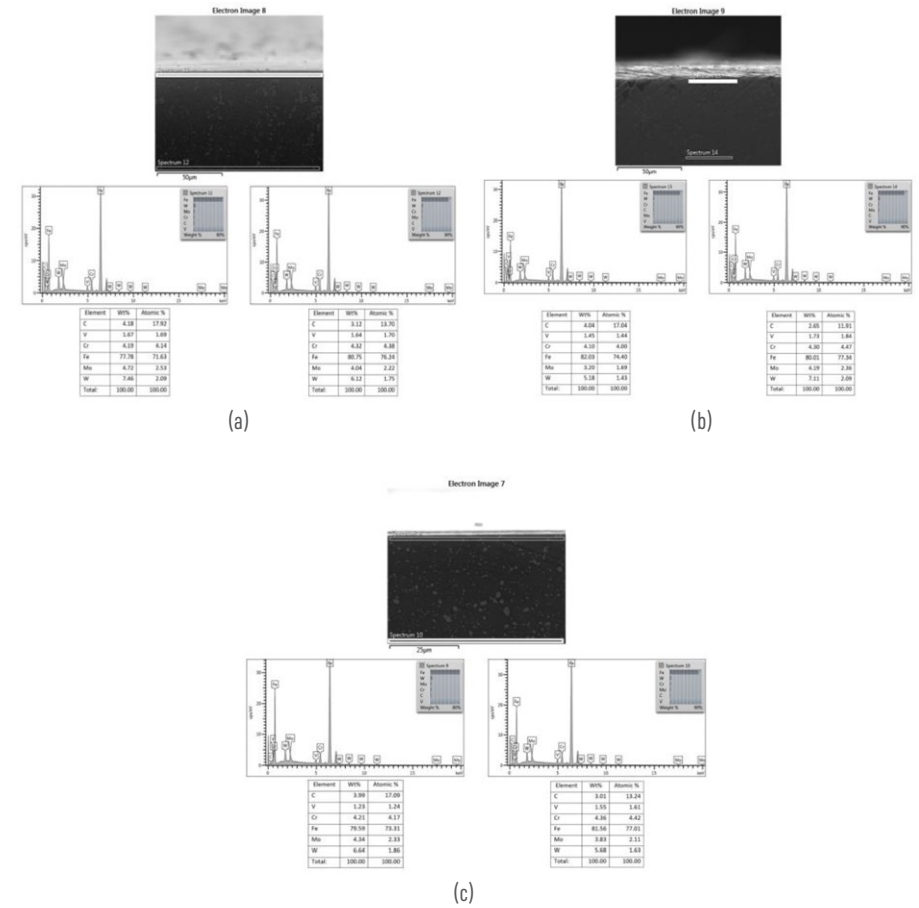


Figure 11. EDS analysis after (a) air cooling, (b) oil cooling and (c) cryogenic cooling.

4. Conclusions

In this study, cryogenic cooling with LN₂ was compared with air and oil cooling mediums for turning of 1.3343 samples. It was proven that cryogenic cooling showed a significant improvement in terms of flank wear with respect to the process parameters. Some of the inserts failed during trials with air and oil cooling mediums. However, no insert failure was encountered in any of the trials with cryogenic cooling.

In terms of surface roughness, machining with cryogenic cooling helps to obtain a better surface finish, especially for more severe cutting conditions. Depending on the production route, a better surface finish after the turning operation can contribute to an increase in productivity such as by decreasing the cycle time per part for the subsequent final polishing operation.

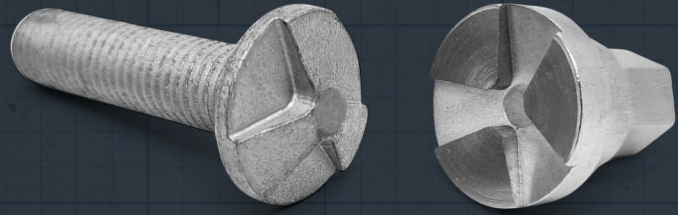
Considering the residual stress measurements, compressive residual stress fields were observed in the direction of machining for all cooling mediums. The most compressive residual stresses were obtained at the surface of the sample machined with oil cooling. Decrease in feed rate leads to more compressive residual stresses for both directions parallel and perpendicular to the machining direction for cryogenic cooling. Compressive residual stress fields can act against crack initiation and propagation leading to better fatigue resistance.

As a result of detailed SEM and EDS analyses, no recast or white layer was found on the surfaces of the machined samples with air, oil and cryogenic cooling.

In addition to the underlined advantages, cryogenic cooling offers more sustainable production particularly compared to oil cooling. Since there is no need for a recycling process as for oil-based coolants, cryogenic cooling can be considered more environmentally friendly.

References

- [1] Aramcharoen, A., 2016, Influence of cryogenic cooling on tool wear and chip formation in turning of titanium alloy, CIRP Conference on High Performance Cutting.
- [2] Hong, S. Y., Zhao, Z., 1999, Thermal aspects, material considerations and cooling strategies in cryogenic machining, Clean Products and Processes 1, 107-116.
- [3] Potta, S., 2018, Effect of cryogenic coolant on turning performance: a comparative study, SN Applied Sciences.
- [4] Agrawal, C. et al., 2020, Tool wear progression and its effects on energy consumption and surface roughness in cryogenic assisted turning of Ti-6Al-4V, The International Journal of Advanced Manufacturing Technology.
- [5] Ayed, Y., 2017, Impact of supply conditions of liquid nitrogen on tool wear and surface integrity when machining the Ti-6Al-4V titanium alloy, The International Journal of Advanced Manufacturing Technology.



A COMPARISON OF STATIC AND FATIGUE PERFORMANCE OF HIGH-STRENGTH BOLTS DEPENDING ON HEAT TREATMENT PROCESS

Dogus ZEREN
Burak HIZLI
Sarper DOĞAN
M. Burak TOPARLI
Umut İNCE



3rd International Materials Technologies And Metallurgy Conference - Imtmc 2023

A COMPARISON OF STATIC AND FATIGUE PERFORMANCE OF HIGH-STRENGTH BOLTS DEPENDING ON HEAT TREATMENT PROCESS

Dogus Zeren¹, Burak Hizli¹, Sarper Dogan¹, M. Burak Toparli¹, Umut Ince¹

¹Norm Civata San. ve Tic. A.Ş., R&D Center, IAOSB 35620 Cigli, Izmir, Turkey

Keywords: High-Strength Bolts, Mechanical Properties, Fatigue, Heat Treatment

Abstract

Fastening products such as high-strength bolts are crucial assembly parts for the automotive industry. In the recent years, environmentally sustainable regulations have led to increasing demand for high-strength bolts in the industry to reduce vehicle weight by lessening the number of fasteners used in the assembly lines. In this study, the static and fatigue properties of the high-strength bolts which were subjected to post-heat treatment combined with varying tempering temperatures and durations were investigated to achieve better durability and higher mechanical properties with desirable ductility. Obtained properties in terms of microstructural, mechanical and fatigue were evaluated. According to the results, it is observed that better mechanical properties are up to 13,6% and 11,6% for yield strength and tensile strength, but deterioration in elongation was around 47,4% compared to 12.9 grade. Additionally, bolts having higher static strength exhibited significantly lower fatigue performance for some load conditions considering the life cycles acquired from 12.9 grade.

1. Introduction

Fasteners are one of the most important parts for assembling the components in the main systems and subsystems that are designed in major industries such as automotive, aviation, construction, white goods, etc. Suitable grade and mechanical properties of fasteners are determined considering the assembly conditions in order to maintain the structural integrity. In the recent years, trends especially in the automotive industry have been encouraging the weight reduction as the transformation to electrical vehicles accelerates and efforts addressed to travelling long distances using less electric energy. Therefore, bolts having higher grades than standard grades described in ISO 898-1 are in demand to ensure reduced size and also reduced quantity of used fasteners in the system for weight reduction purposes [1, 2]. On the other hand, OEMs steadily work on developing smaller engine blocks without sacrificing engine power [3]. Therefore, the necessity of high-strength bolts can clearly come in sight to prevent the adverse conditions and protect the engine block assembly [4]. In addition to these, the usage of high-strength fasteners enables to increase production efficiency in terms of labor savings and more rapid assembly operations [5]. However, there are some issues that restrict the mass production of high-strength bolts.

Fasteners are generally manufactured by cold forming process with post-heat treatment application using low and medium carbon steels as a raw material. Depending on the property grade, additional alloying elements such as B, Mn, and Cr are needed to enhance the strengthening and hardenability of the carbon steels. Especially, boron addition for solid solution allows higher hardenability even at low concentrations, but it raises the tendency to form detrimental compounds such as boron oxide, nitride, and carborites that cause an instability in the quenching process [6].

Therefore, several studies in the literature focused on boron-free steels, mostly 42CrMo4, for reaching higher strength properties due to increased carbide formation and finer grain structure obtained by heat treatment [6-8]. Thus, 42CrMo4 stands in good candidate for manufacturing high-strength bolts with tensile strength up to 1600 MPa [9].

In this study, high-strength bolts with 1400 MPa tensile strength and 12.9 grade bolts produced from 42CrMo4 were heat-treated using different temperature-time combinations as to form tempered martensite microstructure at final. Thereafter, the obtained properties were evaluated in the aspects of microstructural features, mechanical, and fatigue performance. It was witnessed that significant deterioration in fatigue performance and ductility for higher strength grade compared to 12.9 grade, while the strength values increased.

2. Experimental Procedure

M10 bolts having 150 mm length were produced by cold forming process using five-staged bolt former machine and final product form is given in Figure 1. The material used as raw material for this study is 42CrMo4 steel in the wire-drawn form, whose chemical compositions are shown in Table 1.

Table 1. Chemical composition of 42CrMo4 steel.

Element	C	Cr	Mo	Ni	Mn	Si	Fe
wt (%)	0.40	1.1	0.23	≤0.15	0.75	≤0.2	balance



Figure 1. Final bolt form after the production.

Prior to production, spheroidization annealing was applied to steel wires to facilitate the cold forming process by decreasing the hardness values into desired range. Thereafter, surface of the wires were coated with polymer to adjust the frictional effects during cold forming process. As a final process, bolts were subjected to heat treatment under three steps; austenization, quenching, and tempering. Both specimen batches were first austenized and quenched. Following that, high-strength bolts were tempered at different temperatures and durations in order to reach at least 10% elongation without decarburization.

Microstructural observations were conducted on specimens of both grades using Zeiss Axio Imager.M2m optical microscope after metallographic preparations via grinding and polishing, and etching with 4 vol% nital-distilled

water solution for 3-5 s to control the final microstructure and decarburization. Uniaxial tensile tests using special test fixtures with a loading rate of 0,166 mm/s were carried out on Zwick Roell Z400RED universal testing machine for each grade bolts at room temperature to determine the mechanical properties. Three tests from each grade were performed. Additionally, fatigue tests of both grade bolts were carried out on Zwick Roell Amsler 250 HFP 5100 high-frequency fatigue machine at constant mean load and alternating load amplitudes. Mean load value used in fatigue tests was 39,41 kN. Load amplitudes were determined according to the mean load value as not to exceed yield strength of 1080 MPa for 12.9 grade. Five tests from both grades at each load amplitude were performed. Fatigue test parameters are given in Table 3 in detail.

Table 2. Fatigue test parameters.

Mean Load, kN	Cyclic Load, kN	Corresponding % of Mean Load
39,41	7,88	20
	5,91	15
	3,94	10
	1,97	5

3. Results and Discussion

The microstructures of specimens of both grades exhibit transformation to tempered martensite which consists of lath-type structure. Also, it is seen that heat treatment process is successfully completed for all specimens without decarburization. The micrograph of the specimen with tensile strength of 1400 MPa is illustrated in Figure 2.

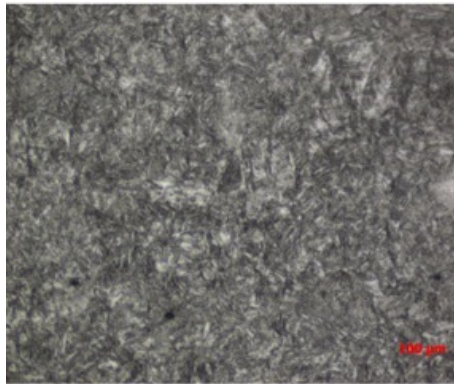


Figure 2. Tempered martensite microstructure without decarburization taken from higher grade bolt.

Mechanical properties of bolts with high-tensile strength are given in Figures 3, 4, and 5 for ultimate tensile strength, yield strength, and elongation at fracture depending on tempering time, respectively. The mechanical strength of the bolts were inversely proportional to fracture at elongation i.e. ductility. The heat treatment process parameters had significant influence on these properties. Therefore, the appropriate combination of temperature-time in tempering process is determined in order to obtain adequate ductility with tensile strength of 1400 MPa or above. Obtained mechanical properties for both grade bolts are listed in Table 4 for comparison the mechanical properties. According to the results, it was observed that as the tempering temperature decreased, better mechanical properties up to 13,6% and 11.6% for yield strength and tensile strength were obtained. However, fracture at elongation was decreased around 47.4% compared to 12.9 grade.

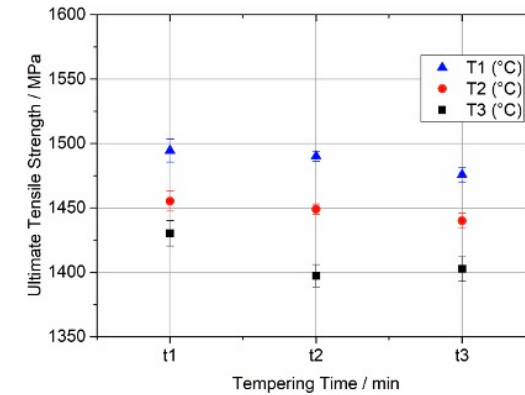


Figure 3. Ultimate tensile strength-tempering process relations.

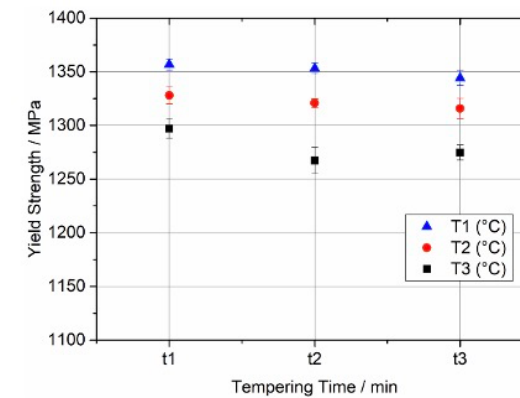


Figure 4. Yield strength-tempering process relations.

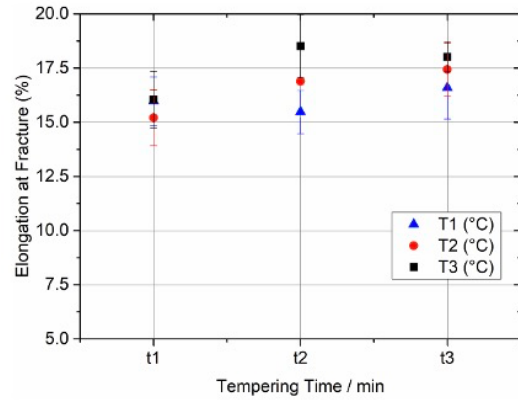


Figure 5. Elongation at fracture-tempering process relations.

Table 4. Mechanical properties of both grades.

Property / Grade	12.9	Higher grade
Yield Strength, MPa	1127 ± 3	1280 ± 8
Tensile Strength, MPa	1263 ± 1	1409 ± 4
Elongation at Fracture	20,9 ± 0,5	11 ± 0,7

Averaged fatigue test results at constant mean load of both grades are listed in Table 5. The endurance limit in fatigue tests was determined as 1.000.000 cycles. Results showed that life cycles substantially increased as the cyclic load decreased. Another important output from fatigue tests was that life cycles of higher grade bolts at cyclic load of 5,91 kN significantly decrease to half of the life cycles obtained from 12.9 grade. Also, it was seen that life cycles of higher grade bolts exhibited lower resistance to fatigue loads compared to 12.9 grade bolts. The reason could be incorporated with the decrease in deformation capability of the material due to increased strength and hardness. Higher strength properties could lead to restriction of dislocation movements and a brittleness in the material structure. Life cycle decrease seen in higher grade tests could be explained by deterioration of ductility and deformability. Though higher grade bolts showed good performance under static loads, their resistance against fatigue loads was lower than 12.9 grade bolts. S-N diagrams of both grade bolts given in Figure 5 and 6, respectively. Considering that fasteners especially used in the automotive industry, which are exposed to repetitive, variable and uncertain loads, it is clear that bolts with low fatigue life are not desirable.

Table 5. Fatigue test results of both grades.

Mean Load, kN	Cyclic Load, kN	Cycles		Difference (%)
		12.9	UTS ≥ 1400 MPa	
39,41	7,88	45.669	42.993	-5,9
	5,91	254.083	121.148	-52,4
	3,94	573.241	614.298	+7,2
	1,97	≥1.000.000	≥1.000.000	-

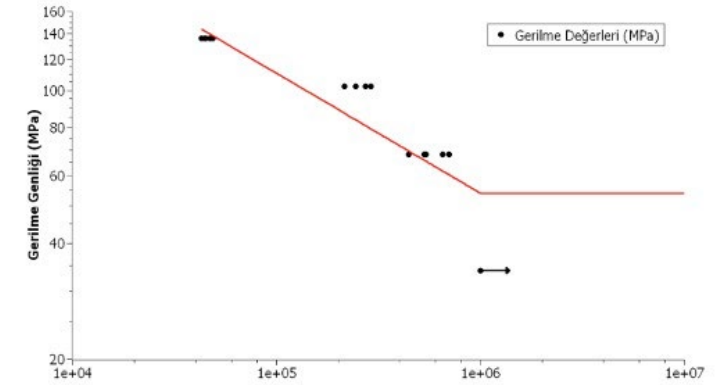


Figure 6. S-N diagram of 12.9 grade bolts.

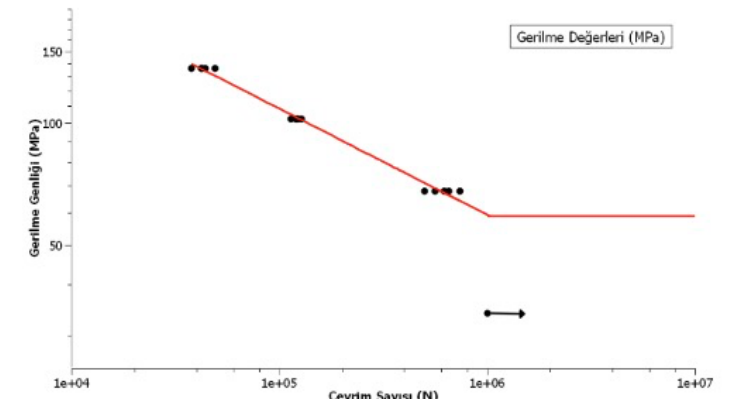


Figure 7. S-N diagram of bolts having 1400 MPa tensile strength.

4. Conclusion

In the scope of this study, the static and fatigue properties of the high-strength bolts which were subjected to post-heat treatment combined with varying tempering temperatures and durations were investigated in order to achieve better structural integrity. The following conclusions can be drawn from this study:

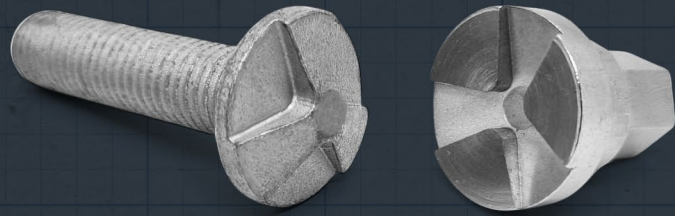
1. Optical microstructure observations indicated that all temperature-time combinations applied in heat treatment provided tempered martensite microstructure at final.
2. According to obtained mechanical properties of both 12.9 grade and higher grade with tensile strength 1400 MPa, yield and tensile strength values were increased by up to 13.6% and 11.6%, however ductility of the material significantly reduced around the ratio of 47.4% compared to 12.9 grade due to increased hardness and loss of deformation capability.
3. Fatigue results of both grades showed that life cycles substantially increased as the cyclic load decreases. Considering the life cycles at relatively high cyclic loads, higher grade bolts exhibit lower resistance to fatigue loads compared to 12.9 grade bolts. Though higher grade bolts show good performance under static loads, their resistance against fatigue loads is lower than 12.9 grade bolts for some load conditions.
4. Bolts with low fatigue life would lead to disadvantageous conditions due to exposing to adverse loads in repetitive, variable and uncertain manner. Despite the better mechanical performance under static loads, high-strength bolts should be use considering lower fatigue resistance.

Acknowledgment

The authors would like to thank Norm Holding for the opportunity to carry out this work.

References

- [1] ISO 898-1:2013; Mechanical properties of fasteners made of carbon steel and alloy steel - Part 1: Bolts, screws and studs with specified property classes - Coarse thread and fine pitch thread, 2013.
- [2] M. Takashima, Iida, Z., Tanaka, S., Tsukiyama, K. et al., "Development of 1600 N/mm² Class Ultra-High Strength Bolts," SAE Technical Paper 2003-01-1179, 2003.
- [3] T. Hamada, Kobayashi, D., Oyanagi, M., Tanabe, T. et al., "Development of Plastic Region Tightening 1.6-GPa Ultra-High Strength Bolt with High Delayed Fracture Resistance," vol. SAE Technical Paper 2019-01-1116, 2019.
- [4] C. Ohlund, M. Luković, J. Weidow, M. Thuvander, and S. Offerman, "A Comparison between Ultra-high-strength and Conventional High-strength Fastener Steels: Mechanical Properties at Elevated Temperature and Microstructural Mechanisms," ISIJ International, vol. 56, pp. 1874-1883, 2016.
- [5] K. Azuma, T. Chida, T. Tarui, N. Matsuishi, and T. Okada, "Development of super high-strength bolts with tensile strengths of 1600 to 2000 N/mm²," International Journal of Steel Structures, vol. 9, no. 4, pp. 291-299, 2009.
- [6] A. Zaitsev et al., "Study of the Effect of Quenching and Tempering Modes on the Strength Level of Alloyed Structural Steels Used to Produce Fasteners," Metals, vol. 12, no. 9, 2022.
- [7] W. Huang, H. Zhong, L. Lei, and G. Fang, "Microstructure and mechanical properties of multi-pass forged and annealed 42CrMo steel," Materials Science and Engineering: A, vol. 831, p. 142191, 2022.
- [8] A. Çalık, O. Dokuzlar, and N. Uçar, "The effect of heat treatment on mechanical properties of 42CrMo4 steel," Journal of Achievements in Materials and Manufacturing Engineering, vol. 98, no. 1, pp. 5-10, 2020.
- [9] H. Lee, Y. Jo, and B. Jang, "Hot Deformation Behavior and Dynamic Recrystallization of a Medium Carbon Cr-Mo Steel for Class 16.8 Bolts," Metals and Materials International, 2023.



WIRE-EDM CUTTING STRATEGIES OF WC-CO HARDMETALS: EFFECT OF NUMBER OF EDM PASS ON SURFACE INTEGRITY

M. Burak TOPARLI



Journal of Process Mechanical Engineering Special Issue: Advances in Processing & Characterisation of Materials DOI: 10.1177/09544089231207741

WIRE-EDM CUTTING STRATEGIES OF WC-CO HARDMETALS: EFFECT OF NUMBER OF EDM PASS ON SURFACE INTEGRITY

M. Burak Toparli^{1,2*}

¹Norm Fasteners San. ve Tic. A.Ş., IAOSB, Cigli, Izmir, Turkey

²Norm Tooling San. ve Tic. A.Ş., IAOSB, Cigli, Izmir, Turkey

M. Burak Toparli, Norm Fasteners San. ve Tic. A.Ş., IAOSB, Cigli, Izmir, Turkey;

Norm Tooling San. ve Tic. A.Ş., IAOSB, Cigli, Izmir, Turkey.

*Corresponding author: Email address: burak.toparli@normfasteners.com

Abstract

In this study, the effect of the number of wire-EDM passes on the surface integrity of WC-Co hardmetals was investigated. As-received doughnut-shaped WC-25 wt%Co samples were wire EDM'ed with one, two, three and five passes. The resulting surface conditions were investigated in terms of macroscopic and microscopic examinations. Surface roughness and hardness measurements were carried out. Detailed SEM investigations were coupled with EDS analyses. Based on the experimental findings, a detailed cutting strategy was offered for WC-Co hardmetals depending on the expectations of surface conditions, production route, cost and productivity. If there is at least one subsequent process including material removal, wire-EDM with one pass is suggested to decrease cost and increase productivity. However, heat-affected zone (HAZ), recast layer and lower surface hardness region should be removed at subsequent production steps. If there are no production steps to remove HAZ, recast layer and lower surface hardness region, the number of wire-EDM passes should be maximised.

Keywords: WC-Co hardmetals; wire-EDM; surface integrity; cutting strategy; recast layer

1. Introduction

WC-Co metal-ceramic composite materials are one of the important engineering materials used in various applications in manufacturing [1]. Tungsten Carbide (WC) particles are sintered with cobalt (Co) binder to have both high wear resistance and high toughness. Owing to studies concentrating on the effects of WC particle size and cobalt content on the final performance of materials, the demand for this material type to be used in different applications has been increasing [2]. Knives, mandrels, punches, drawing and forming dies and inserts are some of the tools made of WC-Co hardmetals and are widely used in different metal shaping processes such as forging and machining [3].

Considering various forms, the manufacturing of final products made of WC-Co is carried out in multiple steps to obtain geometrical shapes within tolerances and desired surface conditions. For instance, the production route starts with rough machining or roughening to obtain an approximate geometry from pre-shaped solid or hollow cylindrical raw materials for cold forging dies made of WC-Co. After roughening, further steps including fine machining, grinding and polishing are employed depending on the final shape and expected surface conditions. Since WC-Co metal matrix composite materials are very hard, required cutting forces are very demanding. Due to high hardness, tool wear and tool cost are

higher and production time is longer compared to machining of conventional steels. Since the machining of hardmetals differs from other materials in terms of operation parameters, a different term, i.e. hard machining, is often used [4].

Owing to the high material removal rate, Electro Discharging Machining (EDM) is one of the widely preferred methods for machining of WC-Co hardmetals. However, different artefacts such as surface cracks, heat-affected zone (HAZ), recast layer, additional surface roughness and tensile residual stresses can be introduced during processing. Based on the literature review on the machining of WC-Co hardmetals, it was concluded that the issues related to the EDM of WC-Co could be attributed to differences in physical properties such as melting and evaporation temperatures, thermal expansion and contraction coefficient and electrical conductivity [5]. EDM is based on high-voltage electrical current passing through an electrode and workpiece. Considering the principle of EDM, where the dielectric fluid enables current to be passed to the workpiece after ionization temperature is reached. The resulting spark removes material from the workpiece so that cutting is carried out. Due to high local temperatures originating from high-voltage sparks, microstructural modifications are introduced during EDM. One of the widely-known features is the recast layer which is a μm -sized layer observed at the surface of the materials. Due to EDM, tensile residual stresses are formed with other inherently-introduced features such as binder depletion and thermal grain cracking lowering the performance of EDM'ed WC-Co hardmetals [6]. It was underlined that ultrasonic vibration of the tool in die sinking-EDM led to a decrease in the thickness of the HAZ and recast layer [7].

Considering the studies focusing on the EDM of WC-Co hardmetals, most of the attention was directed to the effect of EDM parameters, such as applied intensity, pulse time, wire feed rate etc. For example, the effect of pulse time on various WC-Co grades was investigated [8]. It was concluded that an increase in pulse time led to machining instability. The effect of peak current and pulse duration was explored for WC-25wt% Co [9]. At high peak current and pulse duration, EDM-affected layers with cracks were claimed to be observed. The effect of pulse duration, dielectric level, current, flushing pressure and different dielectric fluids on the material removal rate of WC-10wt% Co samples were investigated [10]. Increase in pulse duration, current and flushing pressure were found to lead higher material removal rate. The effects of pulse intensity, pulse duration, duty cycle and open-circuit voltage were examined in order to have low surface roughness, low electrode wear and high material removal rate for WC-6wt%Co samples [11]. It was suggested that low intensity and low pulse duration should be preferred for low surface roughness. On the other hand, high intensity, duty cycle and open-circuit voltage values with low pulse duration should be chosen for high material removal rate. High intensity as well as low open-circuit voltage and pulse values were offered for low electrode wear. A study focused on determining the most influential factors for surface roughness, electrode wear and material removal rate [12]. It was observed that intensity was the most influential factor for all cases within the limits studied in the study. A review study on the EDM of WC-Co hardmetals was carried out to tabulate the EDM process parameters with respect to achieved material removal rate, electrode wear, tool wear rate and surface roughness [5]. Another review study was conducted on the EDM of WC-Co hardmetals [13]. Process parameters such as spark gap, gap voltage, peak current, pulse duration, pulse interval and pulse intensity were discussed. These literature reviews summarized the studies concentrating on EDM process parameters for WC-Co hardmetals.

Multi-pass EDM cutting is one of the procedures that can be applied to reduce or eliminate the effects of single wire-EDM cutting artefacts such as high surface roughness, recast layer and HAZ as well as tensile residual stresses. Initial rough wire-EDM cutting can be followed by one or more fine trim cuttings to achieve desired surface conditions. The process of the multi-pass wire-EDM procedure was explained in detail in [14]. Experimental and statistical analyses were carried out for gamma titanium aluminide material. In this study, one and two passes were used and a selection procedure based on productivity and expected surface roughness was offered. Another study focussed on the effects of multi-pass wi-

re-EDM cutting for Ti-6Al-4V alloy [15]. Rough cutting followed by two additional trim cuttings with different coated EDM wires were investigated. For all wire types, a reduction in surface roughness and recast layer thickness was observed after multi-pass wire-EDM. ANOVA and Taguchi analyses were conducted to determine the influence of process parameters including multi-pass wire-EDM of WC-5.3wt%Co [16]. Investigations on fracture and fatigue behaviour of wire EDM'ed WC-10wt%Co hardmetals were carried out [17]. Multi-pass wire-EDM'ed samples were compared with samples processed with mechanical grinding and polishing. It was revealed that fatigue sensitivity of the wire-EDM'ed specimens was obtained as higher compared to reference cutting due to tensile residual stresses after EDM. However, there was no specific information regarding the details of multi-pass wire-EDM. The wear and adhesion performance of samples after dry blasting and TiN coating applied to samples produced with different EDM passes were investigated [18]. WC-10wt%Co samples were prepared with one, four, five and seven numbers of wire-EDM passes and it was concluded that applying multi-pass wire-EDM up to 5 passes could create fine TiN crystals. However, it was stated that due to the longer process duration of the multi-pass wire-EDM process, it would not be cost-effective. A review study on the EDM of WC and WC-Co suggested multi-pass EDM process with lower depth of cut [19]. However, there was no further information regarding the multi-pass wire-EDM process. In addition, the effect of number of wire-EDM pass on breaking strength obtained by four-point bending test was investigated [20]. It was found that the post-cuts were necessary only to improve surface roughness. It was also stated that decrease in the number of post-cuts would decrease the cost of manufacturing.

Despite some studies mentioning multi-pass wire-EDM of WC-Co hardmetals, a systematic study is needed to explore the resulting changes due to the multi-pass wire-EDM and to suggest cutting strategies that can be implemented on the production floor. In addition, most of the studies in the open literature are concentrating on low Co-content hardmetals, i.e. up to 10wt%. In this study, the effect of wire-EDM passes on surface integrity was investigated for WC-25wt%Co hardmetals. Detailed macro and microstructural examinations were carried out after one, two, three and five passes. After macroscopic examinations, surface roughness and hardness measurements were conducted. Detailed investigations including EDS analysis and microstructural examinations by SEM images were carried out to investigate the surface integrity. Finally, a cutting strategy was offered for wire-EDM cutting of WC-Co hardmetals in terms of surface integrity and production efficiency. Since the final performance of WC-Co hardmetals is directly related to surface integrity, the cutting strategy offered in this study presents the most cost-effective wire-EDM production step, depending on the complete production route without any sacrifice from surface integrity.

2. Sample preparation

In this study, doughnut-shaped WC-Co samples were employed. As received samples were produced from WC and Co powders by milling, powder pressing, preforming and sintering. The inner and outer diameters of the as-received samples were 13.30 mm and 30.80 mm, respectively. The as-received sample was cut into four pieces so that each sample had a thickness of 5.50 mm. The cobalt content of the samples was 25 wt% and the grain size of WC particles was higher than 6 μm . The mechanical and physical properties of WC-Co samples used in this study was given in Tab. 1.

After obtaining four samples with the same geometry, the inner hole size was increased to 14.20 mm by using SPM z-Cut

Table 1. Elemental, physical and mechanical properties of WC-Co material used in this study.

Material	Co Content (%)	Density (g/cm ³)	Grain Size	Elasticity Modulus (GPa)	Transverse Rupture Strength (MPa)	Fracture Toughness (MPa*m ^{1/2})
WC-Co hardmetal	25	13.15	Extra coarse (>6 μm)	450	2700	27

wire-EDM. 0.25 mm-thick brass wires were employed for cutting. For each sample, desired final hole diameter was obtained by one, two, three and five passes. The wire-EDM process has various parameters to control and wire-EDM machines have software and hardware to optimise these parameters and their complex interactions depending on the samples to be cut. Parameter optimization requires a substantial amount of work and is well beyond the scope of this work. Therefore, the wire-EDM parameters were automatically defined and controlled by the wire-EDM machine used in this study depending on the number of passes.

After wire-EDM cutting, each sample was further cut into two pieces to obtain semi-doughnut-shaped samples for each configuration. Then, one of the half pieces of each set was polished for further optical investigations. Since, semi-doughnut-shaped samples were obtained from full doughnut-shaped samples by wire-EDM, both one and five passes regions can be seen simultaneously in Fig. 1.

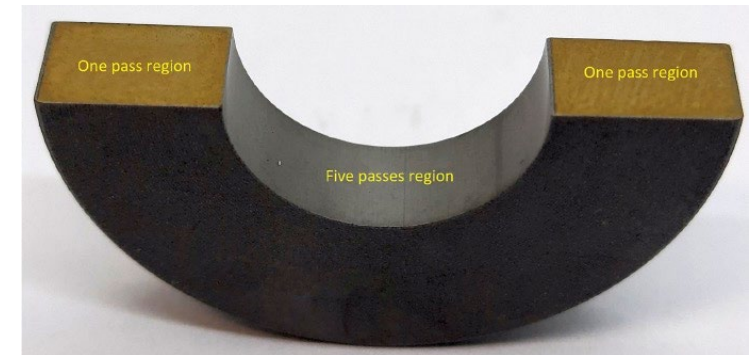


Figure 1. Wire-EDM'ed and polished semi-doughnut-shaped sample after five EDM passes. The Doughnut-shaped sample was cut into two halves by wire-EDM. Therefore, one pass (thickness) and five passes (inner-hole) regions can be seen simultaneously.

3. Methods

Macroscopic examinations were initially carried out for all samples. Surface roughness measurements were carried out by Mitutoyo SurfTest SJ-400. For each configuration, measurements were repeated three times and standard deviations were obtained. Micro hardness measurements were carried out by employing KB 30S and tests were repeated five times. The SEM images were obtained by Carl Zeiss 300VP. Only as wire-EDM'ed samples were used and detailed surface images were recorded from different locations of samples with different wire-EDM passes. EDS analyses were also carried out to investigate the elemental composition of the recast layer formed after wire-EDM.

4. Results & Discussions

4.1. Macroscopic Examinations

Macroscopic examinations were carried out for wire-EDM'ed and polished samples (Fig. 2). Optical investigations revealed critical information regarding the effect of pass. First of all, after a rough polishing, i.e. cleaning the samples from residues of the wire-EDM process, a yellowish recast layer was observed very clearly at the processed surface of the samples with one and two passes. For the wire-EDM'ed sample after three passes, a yellowish recast layer was still observed. Based on macroscopic examinations, the five-passes sample was almost free from the yellowish recast layer. Therefore, as the number of EDM passes was increased, the yellowish layer formed during wire-EDM faded away.

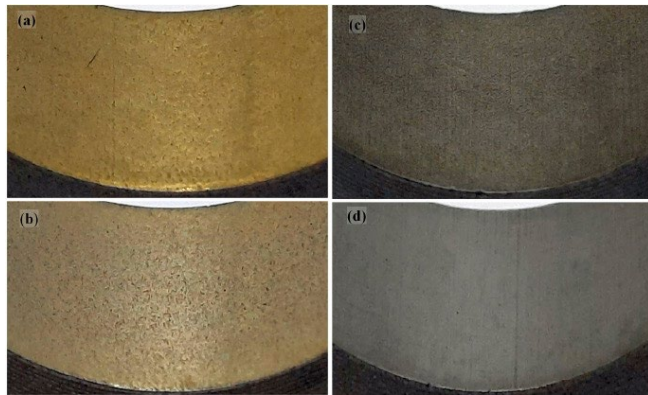


Figure 2. Surface appearance of wire-EDM'ed and polished samples after (a) one, (b) two, (c) three and (d) five passes.

4.2. Surface Roughness

According to surface roughness measurements, it was revealed that both R_a and R_z values were significantly affected by the number of passes. Fig. 3 shows the average R_a and R_z values with corresponding standard deviations for the as-received sample as well as one, two, three and five passes samples. First of all, the average surface roughness values of the as-received sample were measured as 2.04 and 12.30 μm for R_a and R_z , respectively. The average surface roughness values after one pass, i.e. R_a and R_z , were increased to 4.07 and 22.56 μm , respectively. The percent increase after one pass was 99 and 83% for R_a and R_z values compared to the as-received sample. Therefore, it was revealed that surface roughness significantly increased for the one-pass sample. When the two-passes sample was investigated, R_a and R_z values were decreased to 3.35 and 18.38 μm compared to the one-pass sample, however, surface roughness values were still higher compared to the as-received sample. For the three-passes sample, surface roughness values were obtained as 0.83 and 5.86 μm for R_a and R_z respectively. Therefore, after three passes, the surfaces started to be smoother compared to the initial conditions of the as-received sample. The percent decreases in R_a and R_z values of the three-passes sample were about 59 and 52%, respectively. Considering macroscopic examinations given in Fig. 1, the dramatic surface roughness

change from two passes to three can also be incorporated with the change in colour of the recast layer. Finally, R_a and R_z values were obtained as 0.42 and 3.32 μm , after five passes. The percent decrease in R_a and R_z from three passes to five passes was about 49 and 43%. The total surface roughness improvements from the as-received sample to the five-passes sample were around 79 and 73% for R_a and R_z , respectively. Based on the surface roughness measurements, it was shown that for the one and two-passes samples, the surface roughness values were increased compared to the as-received sample. However, after three passes, the surface roughness values started to decrease leading to a better surface finish. When the number of passes was five, significant improvements in terms of R_a and R_z were achieved. Therefore, to improve the surface integrity after wire-EDM, the number of passes should be increased to at least three, based on the set-up used in this study. If the number of passes is lower, surface roughness should be decreased with a subsequent process such as polishing. As known, high surface roughness increases the probability of crack initiation leading to a lower performance for fatigue. Therefore, surface roughness should be decreased for better surface integrity, particularly against fatigue failures.

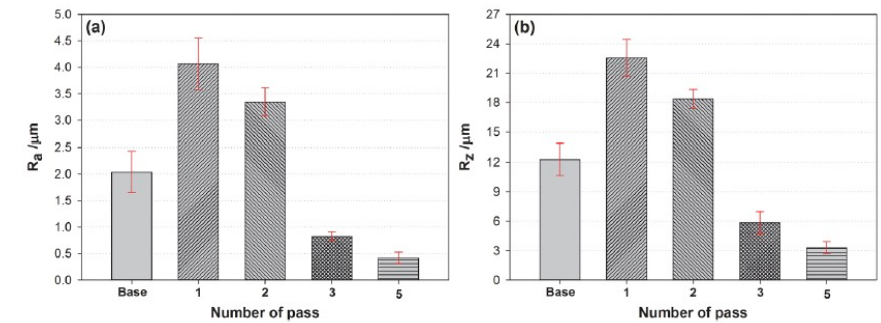


Figure 3. (a) R_a and (b) R_z surface roughness measurements of wire-EDM'ed samples.

4.3. Hardness

Micro-hardness measurements were obtained from wire-EDM'ed surfaces. The as-received sample had an average hardness of 834 HV as can be seen in Fig. 4. The one-pass sample showed a significant reduction of 44% in hardness. The main reason for the hardness decrease was associated with the recast layer after wire-EDM. Since WC-Co materials are very hard, it was shown that the recast layer has lower hardness compared to the base material. As the number of passes increased, the surface hardness also increased. For the five-passes sample, surface hardness was obtained very close to that of the as-received samples. As shown in this study, processing with a low wire-EDM pass causes a decrease in the hardness of WC-Co ma-

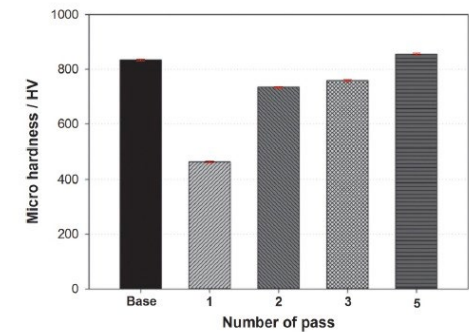


Figure 4. Surface micro-hardness measurements of wire-EDM'ed samples.

materials. Therefore, premature failures can be observed due to hardness decrease at the surface of the material. As a result, performance loss can be expected as a result of lower hardness values for applications such as cold forging dies, where surface hardness is very important to increase wear resistance.

4.4. SEM and EDS Analysis

Detailed microstructural examinations were carried out by using SEM for the as wire-EDM'ed samples without any polishing. After one pass, the so-called recast layer (the yellowish layer for macro examination) was observed at the processed surface (Fig. 5). The average thickness of the layer was about 12 μm . In addition to the recast layer, the heat-affected zone (HAZ), as seen in welding operations, was also observed. The thickness of the HAZ was about 20 μm . Therefore, the average thickness of the wire-EDM-affected zone for the one-pass sample was about 35 μm . Similar to the HAZ seen in this study, a so-called "damaged layer" was observed in the literature [9]. When the as wire-EDM'ed sample with two passes was investigated, the average thickness of the recast layer was obtained as 8 μm . No significant HAZ was observed compared to the sample with one pass. For the three-passes sample, the recast layer was still observed with an average thickness of 5 μm . And similar to the two-passes sample, no significant HAZ was observed. As for the five-passes sample, there were still local recast layers observed at particular locations and there were some regions with no recast layer. Therefore, SEM image analysis revealed that after one pass, a significant recast layer and HAZ were obtained. With the increase in the number of passes, the thickness of the recast layer was decreased with no significant heat-affected region. After five passes, the recast layer started to be diminished, however, there were some locations with very thin and local recast layers. The main mechanism for the formation of the recast layer and HAZ can be interrelated with the sudden temperature increase and decrease during wire-EDM cutting. Due to the heating and cooling cycle taking over a very short period, cracking was also observed at HAZ, which is also similar to HAZ cracking observed in welding (Fig. 6). This subsurface cracked region is very detrimental to the service life of the parts that are particularly working under loading. Therefore, the recast layer and HAZ should be removed for better surface integrity.

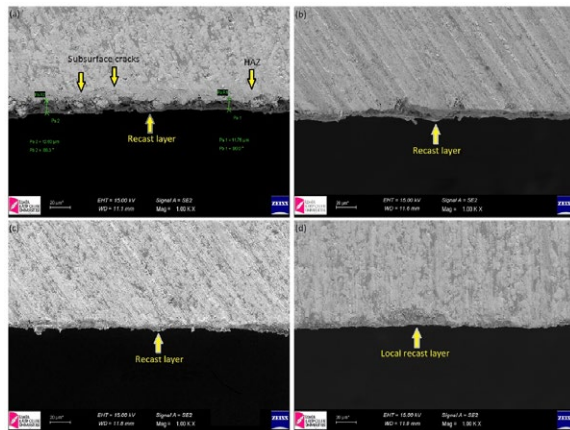


Figure 5. Cross-sectional SEM images of samples with (a) one, (b) two, (c) three and (d) five wire-EDM passes.

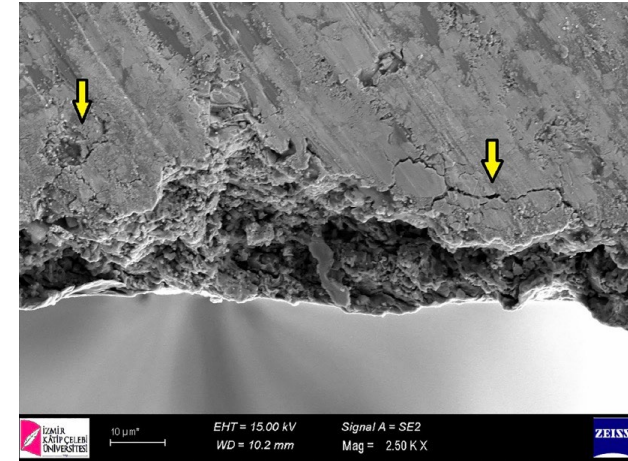


Figure 6. Cracking (shown with arrows) observed at heat-affected zone (HAZ) for one-pass sample.

Along with SEM images, EDS analyses were also conducted to understand the effect of the EDM passes and the mechanism of formation of the recast layer. As shown in Fig. 7, four areas and one spot EDS analyses were conducted on the one-pass sample. The initial area scan (named as Selected Area 1) was selected so that elemental analysis was obtained at the recast layer. Based on EDS analysis on Selected Area 1, significant amounts of Cu and Zn were observed at the recast layer. Since EDM cuttings were conducted with 0.25 mm thick brass (an alloy of Cu and Zn) wires, it was revealed that the recast layer was formed due to the deposition of brass alloy on the cutting surface during wire-EDM cutting. Therefore, it can be concluded that the colour of the formed layer after wire-EDM cuttings, known as the recast layer, originated from the brass wire used in the wire-EDM processes (Fig. 1). The recast layer consisting of mostly Cu and Zn was also the main reason for hardness decrease as obtained in Fig. 4. In addition to Cu and Zn, there were W and C peaks due to WC phase in the base material. Considering initial particle morphology and high temperatures during EDM cutting, it can be inferred that WC particles are melted and solidified in a very short time scale and formed the recast layers with Cu and Zn. Moreover, there was no Co peak recorded from Selected Area 1. The main reason can be attributed to the lower melting and evaporation temperatures of cobalt compared to WC [8]. During wire-EDM, it was stated that cobalt could reach the evaporation temperature before melting of WC particles. Therefore, a cobalt-free region can be formed during wire-EDM.

Another area from the recast layer, named as Selected Area 2, was analysed. Similar elements were observed as compared to Selected Area 1. An additional area was investigated from the HAZ, named as Selected Area 3. The weight percent of Cu and Zn decreased significantly compared to Selected Area 1 and Selected Area 2. On the other hand, the percent of W was increased and significant Co content was obtained. Therefore, it can be inferred that residues of wire in terms of elements were very slight at the HAZ. The final area labelled as Selected Area 4 from the HAZ was analysed and similar elemental composition was obtained compared to Selected Area 3. The point analysis labelled as "EDS Spot 1" was conducted at the cracked region at the HAZ. Elemental analysis showed significant Cu and Zn content in addition to W and C, i.e. very close to the elemental distribution observed at the recast layer with very slight Co content.

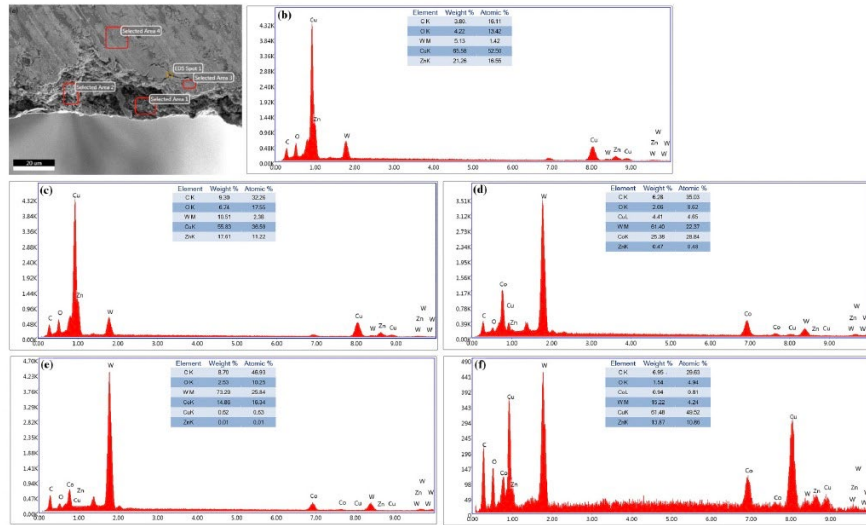


Figure 7. (a) EDS locations of one-pass sample. Intensity and percentage of elemental results of locations as depicted in (a): (b) Selected Area 1, (c) Selected Area 2, (d) Selected Area 3, (e) Selected Area 4 and (f) EDS Spot.

4.5. Wire-EDM Cutting Strategies for WC-Co Hardmetals

In order to determine the wire-EDM cutting strategy of WC-Co hardmetals for a particular application, the production route should be taken into account. Depending on the processes after wire-EDM cutting and desired surface conditions, the number of EDM passes should be determined. In addition, due to tight tolerances expected from particularly tools and inserts made of WC-Co hardmetals, the amount of material to be removed at each step should be projected before production. Moreover, considering the running costs and productivity, parameters such as material removal rate and wire consumption should also be taken into account. The flowchart of the cutting strategies of WC-Co hardmetals offered in this study is given in Fig. 8.

First of all, cracking, recast layer and heat-affected zone (HAZ) observed after one pass should be removed for better surface integrity. Therefore, if there is no further production step in terms of material removal for the wire-EDM'ed surface such as grinding, the number of passes should be maximised. As shown in this study, there were local recast layer zones and residues after five passes. Therefore, after wire-EDM cutting with a maximum number of passes, polishing is suggested to be applied to ensure that all residues of the recast layer are removed. In addition, surface hardness was affected by the number of EDM passes. Decrease in surface hardness was observed for the samples with lower passes. To recover the surface hardness of WC-Co hardmetals, the number of EDM passes should be maximised.

Increasing the number of passes enhances surface integrity, as proven in this study. However, as higher number of passes is employed in serial production, increase in wire-EDM processing time per part and increase in running costs such as wire consumption are inevitable. Therefore, the cost of the wire-EDM process, i.e. the cost of the production will be higher and the productivity will be lower. Therefore, if the production steps after wire-EDM cutting include grinding, i.e. material removal is possible, wire-EDM cutting can be conducted with one pass. However, in the subsequent processes, material removal should be conducted so that the recast layer and HAZ are completely removed from the wire-EDM'ed surface. The thickness of this area was proven to be about 35 μm for the material-EDM set-up used in this study. In addition, surface hardness decrease should be avoided due to one pass. Therefore, while creating a production plan, material removal at each production step should be considered and after wire-EDM cutting with one pass, enough material should be grinded and polished to obtain the final dimensions of the machined part. Hereby, the final surface can be obtained without recast layer, HAZ and lower surface hardness region.

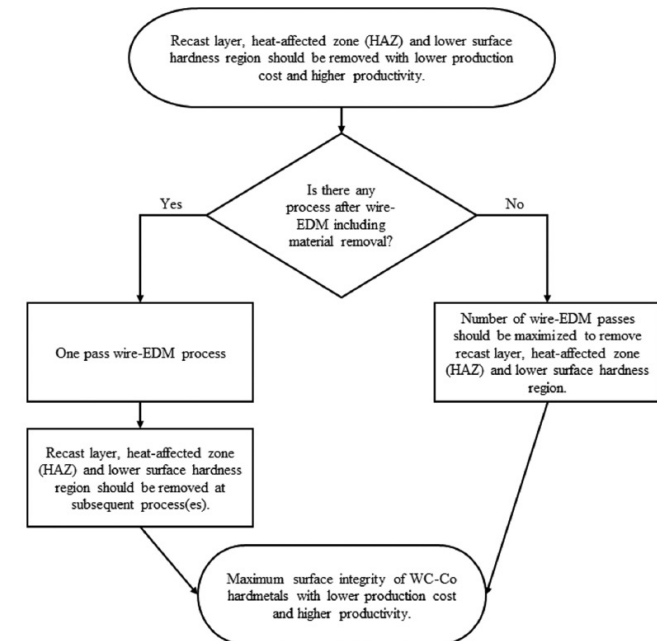


Figure 8. Flowchart of the wire-EDM cutting strategy of WC-Co hardmetals for maximum surface integrity with lower production cost and higher productivity.

In terms of surface roughness, an increase in the number of EDM passes leads to a better surface finish. As shown in this study, an average Ra of 0.42 μm can be obtained with wire-EDM cutting with five passes. Depending on the application, better surface quality can even be achieved by combining multi-pass wire-EDM with applying subsequent processes such as polishing. For some complex-shaped parts, grinding and polishing could be very difficult to apply. In these cases, the number of passes can be maximised to achieve desired surface conditions. However, depending on the expectations from the surface quality, an increase in the number of passes may not be sufficient.

5. Conclusions

Based on this study, the following conclusions can be drawn:

1. A yellowish recast layer was found on the surfaces of wire-EDM'ed samples. As the number of passes increased, the thickness of the recast layer decreased, i.e. yellowish recast layer faded away as the number of passes increased.
2. Surface roughness values were observed to be decreased with increase in number of passes from one to five. However, after one and two passes, the surface roughness values were higher compared to the as-received condition.
3. Surface micro-hardness values after one pass decreased significantly due to the recast layer. Increase in the number of passes led to increase in micro-hardness reaching the as-received sample hardness value.
4. The effect of the number of passes on the surface integrity of processed materials was very significant. The heat-affected zone (HAZ) with micro-cracks observed after one pass can cause premature failures during service conditions. The tendency of observation of the recast layer decreased with increase in the number of passes. Considering the set-up used in this study, there were some recast layer zones even after five passes.
5. Depending on the expectations from surface integrity, the production route should be determined including the number of wire-EDM passes. Surface quality, running costs, productivity should be taken into account and depending on each case, production planning should be made. The cutting strategy offered in this study can be implemented for the production of any parts made of WC-Co hardmetals including wire-EDM.

Acknowledgement

The author would like to thank Norm Holding for the opportunity to carry out this work. All the work was carried out by the Author.

Declaration of conflicting interests

The author declared no potential conflicts of interest with respect to the research, authorship, and/or publication of this article.

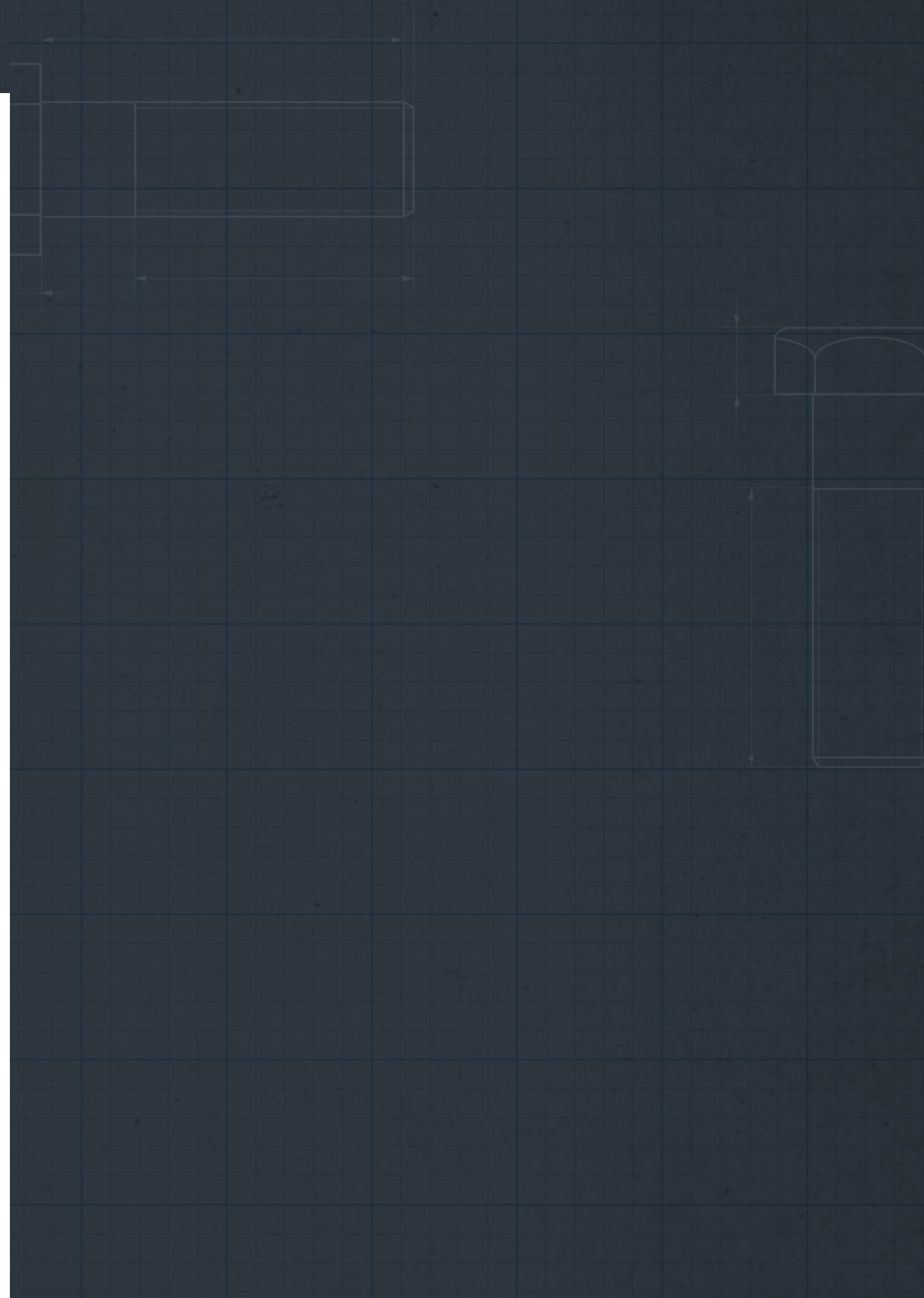
Funding

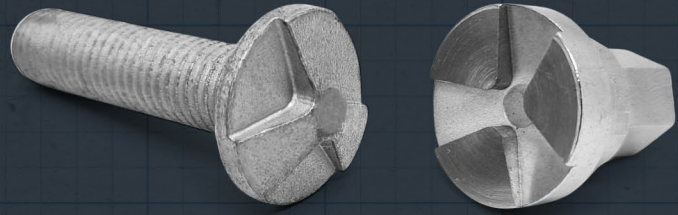
The author received no financial support for the research, authorship, and/or publication of this article.

References

- [1] García J, Collado Ciprés V, Blomqvist A, Kaplan B. Cemented carbide microstructures: a review. *International Journal of Refractory Metals and Hard Materials*. 2019;80:40-68.
- [2] Yang J, Odén M, Johansson-Jöesaar MP, Llanes L. Grinding Effects on Surface Integrity and Mechanical Strength of WC-Co Cemented Carbides. *Procedia CIRP*. 2014;13:257-63.
- [3] Yang J, Roa JJ, Schwind M, Odén M, Johansson-Jöesaar MP, Llanes L. Grinding-induced metallurgical alterations in the binder phase of WC-Co cemented carbides. *Materials Characterization*. 2017;134:302-10.
- [4] Astakhov VP. Machining of Hard Materials – Definitions and Industrial Applications. In: Davim JP, editor. *Machining of Hard Materials*. London: Springer London; 2011. p. 1-32.
- [5] Kataria R, Kumar J. Machining of WC-Co Composites - A Review. *Materials Science Forum*. 2015;808:51-64.
- [6] Tamura T. Development of on-the-Machine Surface Modification Technology in EDM. *Procedia CIRP*. 2013;6:117-22.
- [7] Shabgard MR, Ivanov A, Rees A. Influence of EDM machining on surface integrity of WC-Co. In: Menz W, Dimov S, Fillon B, editors. *4M 2006 - Second International Conference on Multi-Material Micro Manufacture*. Oxford: Elsevier; 2006. p. 331-4.
- [8] Mahdavinnejad RA, Mahdavinnejad A. ED machining of WC-Co. *Journal of Materials Processing Technology*. 2005;162-163:637-43.
- [9] Lee SH, Li X. Study of the surface integrity of the machined workpiece in the EDM of tungsten carbide. *Journal of Materials Processing Technology*. 2003;139:315-21.
- [10] Singh J, Sharma RK. Assessing the effects of different dielectrics on environmentally conscious powder-mixed EDM of difficult-to-machine material (WC-Co). *Frontiers of Mechanical Engineering*. 2016;11:374-87.
- [11] Puertas I, Luis CJ. Optimization of EDM conditions in the manufacturing process of B4C and WC-Co conductive ceramics. *The International Journal of Advanced Manufacturing Technology*. 2012;59:575-82.
- [12] Puertas I, Luis CJ, Álvarez L. Analysis of the influence of EDM parameters on surface quality, MRR and EW of WC-Co. *Journal of Materials Processing Technology*. 2004;153-154:1026-32.
- [13] Bhadauria G, Jha SK, Roy BN, Dhakry NS. Electrical-Discharge Machining of Tungsten Carbide (WC) and its composites (WC-Co) - A Review. *Materials Today: Proceedings*. 2018;5:24760-9.
- [14] Sarkar S, Ghosh K, Mitra S, Bhattacharyya B. An Integrated Approach to Optimization of WEDM Combining Single-Pass and Multipass Cutting Operation. *Materials and Manufacturing Processes*. 2010;25:799-807.

- [15] Khan SA, Usman M, Pervaiz S, Saleem MQ, Naveed R. Exploring the feasibility of novel coated wires in wire EDM of Ti-6Al-4 V aerospace alloy: a case of multi-pass strategy. *Journal of the Brazilian Society of Mechanical Sciences and Engineering*. 2021;43:273.
- [16] Jangra KK. An experimental study for multi-pass cutting operation in wire electrical discharge machining of WC-5.3% Co composite. *The International Journal of Advanced Manufacturing Technology*. 2015;76:971-82.
- [17] Casas B, Torres Y, Llanes L. Fracture and fatigue behavior of electrical-discharge machined cemented carbides. *International Journal of Refractory Metals and Hard Materials*. 2006;24:162-7.
- [18] Sireli E, Orhon N, Sireli GK. Effects of wire-electro discharge machining process on surface integrity of WC-10Co alloy. *International Journal of Refractory Metals and Hard Materials*. 2017;64:190-9.
- [19] Jahan MP, Rahman MA, Wong YS. A review on the conventional and micro-electrodischarge machining of tungsten carbide. *International Journal of Machine Tools & Manufacture*. 2011;51:837-58.
- [20] Juhr H, Schulze HP, Wollenberg G, Künanz K. Improved cemented carbide properties after wire-EDM by pulse shaping. *Journal of Materials Processing Technology*. 2004;149:178-83.





PASLANMAZ ÇELİK CIVATALARIN KOROZYON DİRENÇLERİNİN İNCELENMESİ

Doğuş ZEREN
M. Burak TOPARLI
Samed ENSER
Umut İNCE



The 5th International Conference of Materials and Engineering Technology - TICMET'23

PASLANMAZ ÇELİK CIVATALARIN KOROZYON DİRENÇLERİNİN İNCELENMESİ

DOĞUŞ ZEREN¹, M. BURAK TOPARLI^{1*}, SAMED ENSER¹, UMUT İNCE¹

¹ Norm Fasteners, Ar-Ge Merkezi, AOSB, Çiğli, İzmir, Türkiye

Özet

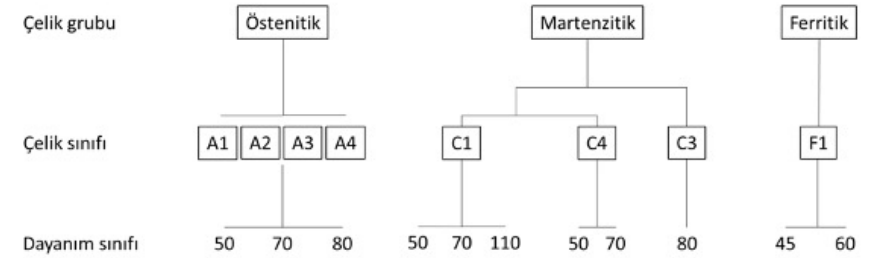
Yüksek sıcaklık başarımları, korozyon dirençleri ve üstün mekanik özellikleri nedeniyle paslanmaz çelikler, imalat sektöründe oldukça fazla kullanılmaktadır. Paslanmaz çelik bağlantı elemanlarına olan ihtiyaç ve talep de günden güne artmaktadır. Denizcilik sektöründe oldukça yaygın olan paslanmaz çelik bağlantı elemanları, günümüzde araçların değişken ortamlara ve tuz gibi korozyon açısından riskli ortamlara maruz kaldığı göz önünde bulundurulduğunda otomotiv sektöründe de oldukça ilgi görmeye başlamıştır. Paslanmaz çelikler, içerdikleri yüksek oranda krom sayesinde, yüzeylerinde oluşan krom oksit tabakası vasıtasıyla korozyon direnci sağlarlar. Ancak yüzeydeki krom oksit tabakası soğuk şekillendirme gibi deformasyonla üretim yapılan durumlarda zarar görür ve korozyona açık hale gelirler. Paslanmaz çeliklerin yüksek korozyon dayanımını tekrar kazanabilmesi için pasivasyon işlemi yapılmaktadır. Bu çalışmada, M10x25 DIN912 paslanmaz çelik civataların pasivasyon işlemi öncesi ve sonrası korozyon dayanımları incelenmiştir. Ayrıca orta karbonlu çelik civatalara korozyon direnci için uygulanan iki farklı ticari çinko lamelli kaplama da paslanmaz çeliklere uygulanabilirliği ve korozyon başarımlarının incelenmesi adına uygulanmıştır. ISO 9227 standardına göre tuz püskürtme testleri gerçekleştirilmiştir. Toplamda dört farklı paslanmaz çelik konfigürasyonunun denemesi tamamlanmış ve sonuçlar karşılaştırılarak değerlendirilmiştir. Sonuç olarak, soğuk şekillendirme ile üretilen paslanmaz çelik civatalar için pasivasyon işleminin beklenen korozyon direncinin elde edilmesinde kritik bir işlem olduğu ortaya konmuştur.

Anahtar Kelimeler: Civata, Soğuk şekillendirme, Paslanmaz çelik, Korozyon

1. Giriş

Paslanmaz çelikler otomotiv, sağlık, havacılık, denizcilik gibi birçok sektörde üstün korozyon dirençleri ve mekanik özellikleri nedeniyle kullanılmaktadır. Hammaddenin daha bulunabilir ve maliyetlerinin düşmesiyle günümüzde daha sık kullanılmaya başlanmıştır. Sektördeki bu kullanım artışından paslanmaz çelik civalar da etkilenmiştir. Östenitik paslanmaz çelikler, en sık kullanılan paslanmaz çelik alaşımlardır [1, 2]. Soğuk şekillendirme ile üretilen paslanmaz çelik bağlantı elemanlarının üretiminde de form verilebilirlik, iş sertleşmesi kabiliyetleri, bulunabilir ve maliyetlerinin görece uygun olması sebebiyle sıklıkla tercih edilen paslanmaz çelik sınıfı östenitik paslanmaz çeliklerdir. Paslanmaz çelik civalar ISO 3506-1 standardı altında sınıflandırılmıştır. Bu sınıflandırmaya göre A sınıfı civatalar östenitik paslanmaz çelikleri ifade etmektedir. Sayıyla belirtilen kısım ise mekanik sınıfını belirtmektedir ve bu değer in on katı çekme dayanımını ifade etmektedir [3].

Paslanmaz çeliklerin içerisinde bulunması gereken en az % 10,5 oranındaki krom ve diğer alaşım elementleri olan nikel, molibdenyum gibi elementler korozyon direncini sağlar. Paslanmaz çeliğin korozyon direnci, yüzeyinde çelik oksijene maruz kaldığında doğal olarak oluşan ince bir krom oksit tabakasının varlığından kaynaklanmaktadır. Bu

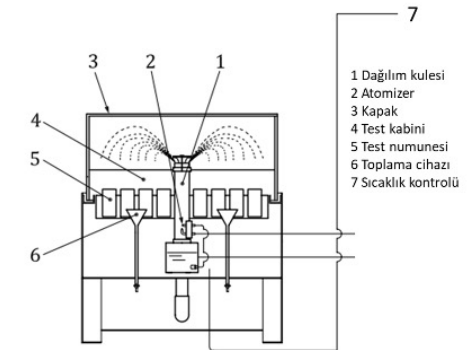


Şekil 1. Civatalar için paslanmaz çelik kaliteleri ve özellik sınıfları tanımlama sistemi [3].

katman, oksijen ve diğer aşındırıcı maddelerin çeliğe nüfuz etmesini ve alttaki metale ulaşmasını engelleyen bir bariyer görevi görür. Soğuk dövme sonrası bu krom oksit tabakasında hasar oluşumu veya kontamine olma durumu, bu oksit tabakasının korozyon direncini düşürmesine sebebiyet verebilmektedir [4]. Bunun önüne geçebilmek için paslanmaz çelik bağlantı elemanlarına pasivasyon işlemi uygulanmaktadır. Pasivasyon işlemi ASTM tarafından A 967-05 belgesinde standardize edilmiştir [5].

Paslanmaz çelikler her ne kadar korozyona dayanıklı olsa da, tamamen korozyona dayanıklı değildir. Gerilmeli korozyon, erozyon, galvanik korozyon, oksidasyon, çukurcu korozyonu gibi korozyon tipleri paslanmaz çeliklerde karşılaşılan korozyon türleridir. Çelik bağlantı elemanlarının korozyon özelliklerinin belirlenmesine yönelik çalışmalar ve testler mevcuttur. Tuz püskürtme testleri sert ortam koşullarını simüle etmesi sayesinde belirli bir standarda göre yapıldığından ötürü sonuçların tekrarlanabilirliği ve hızlı sonuç alınabilmesi açısından önemli bir test metodudur. Paslanmaz çelik bağlantı elemanları zorlu ortamlarda kullanılabilirdiğinden ötürü uygulanan tuz püskürtme testleri de korozyon direnci açısından bilgi vericidir. Tuz püskürtme testleri ISO 9227 ile standardize edilmiştir [6].

Paslanmaz çelik üretiminin artması ve paslanmaz çelikten üretilen civataların yaygınlaşmasıyla beraber mekanik ve kimyasal özellikler açısından bir bilgi ve tecrübe açığı oluşmuştur. Bu nedenle, literatürde paslanmaz çelik civatalar



Şekil 2. Tuz püskürtme kabini tasarımının şematik diyagramı [6].

ile alakalı akademik çalışmalar günden güne artmaktadır. 2007 yılında yapılmış bir çalışmada 304 paslanmaz çeliklerin magnezyum klorit çözeltisi damlatılarak çukurcuk korozyonu oluşumu incelenmiş ve bu sayede deniz atmosferi altında paslanmaz çeliklerin korozyona uğrama mekanizmalarını araştırmışlardır. Damla çapı azaldıkça korozyon oluşma olasılığı ve oluşan çukurcuk korozyonlarının çaplarının da düşmekte olduğu bildirilmiş ve ayrıca klorür çözeltilerinin damlacıkları altında oluşan çukurcukların sıg bir tip olduğu, çukurun tercihen yatay yönde ilerlediğini belirtmiştir [7]. Bir başka çalışmada, standart ve Hollo-Bolt paslanmaz çelik civataların sabit genlikte bir yük altında yorulma performansı incelenmiştir [8]. Diğer bir çalışmada ise 304 paslanmaz çelik malzemeden soğuk şekillendirilmesi zor bir formun üretim denemeleri gerçekleştirilmiştir. Hammaddenin 200 °C dereceye ısıtılarak yapılan üretim denemelerinde yüksek iş sertleşmesi gösteren paslanmaz çeliğin işlenebildiğini ortaya koymuşlardır [9]. 2023 yılında yayınlanmış bir başka makalede ise, martenzitik ve östenitik olmak üzere iki farklı paslanmaz çelik civatanın iki farklı kaplama uygulanarak torklama testleri gerçekleştirilmiş ve kaplama tiplerinin paslanmaz çeliklerde torklama üzerindeki etkisi araştırılmıştır. Çalışma sonunda kaplamaların torklama üzerindeki etkisi belirlenmiş ve istenilen sürtünme katsayı aralığının yakalanabilmesi adına kaplama uygulamalarının gerekli olduğu yorumu yapılmıştır [10].

Bu çalışmada Norm Fasteners bünyesinde üretilmiş M10x25 DIN912 A2-70 sınıfı paslanmaz çelik inbus civataların korozyon özellikleri araştırılmıştır. Civatalar doğrudan üretildiği gibi, pasivasyon işlemi gerçekleştirilmiş ve ticari iki farklı çinko lamelli kaplama ile kaplanmış olacak şekilde toplamda dört farklı koşulda ISO 9227 standardına göre tuz püskürtme testi gerçekleştirilmiştir. Tuz püskürtme testleri sayesinde hem pasivasyonsuz hem pasivasyonlu, hem de farklı kaplama tiplerine sahip bağlantı elemanlarının korozyon dirençleri belirlenmiştir.

2. Materyal ve Metot

Norm Fasteners Ar-Ge Merkezi'nde gerçekleştirilen çalışma kapsamında, test için kullanılan M10x25 DIN912 paslanmaz çelik civatalar Norm Fasteners bünyesinde üretilmiştir. A2-70 sınıfı üretilen civataların üretiminde 304Cu hammadde kullanılmıştır. Kullanılan hammaddenin kimyasal kompozisyonu Tablo 1'de verilmiştir.

Table 1. 304Cu hammadde kimyasal kompozisyonu.

Element	C	Si	Mn	P	S	Cr	Ni	Cu
Oran (w/w)	0.017	0.25	0.77	0.035	0.001	18.15	8.06	3.51

Testlerde kullanılacak M10x25 DIN912 A2-70 paslanmaz test civatalarının üretilmiş son halleri Şekil 4'te gösterilmiştir. Soğuk dövme ile üretimi tamamlanan civatalar tarak kalıpları kullanılarak diş açılmıştır. Ardından, test için hazırlanan numuneler yağ gibi üretimden kaynaklanan kontaminasyonlardan arındırılmıştır.

Korozyon direncini artırmak adına üretimi yapılmış olan M10x25 DIN912 civatalara ASTM A-967 standardına uygun olacak şekilde pasivasyon işlemi yapılmıştır. Krom, paslanmaz çeliğin yüzeyinde, alttaki metali korozyondan koruyan pasif bir oksit tabakası oluşturur. Bu oksit tabakası, alttaki metali korozyona maruz bırakabilecek soğuk dövme, talaşlı imalat gibi işlemler sırasında hasar görebilir veya kirlenebilir. Bu durumlarda, oksit tabakasını eski haline



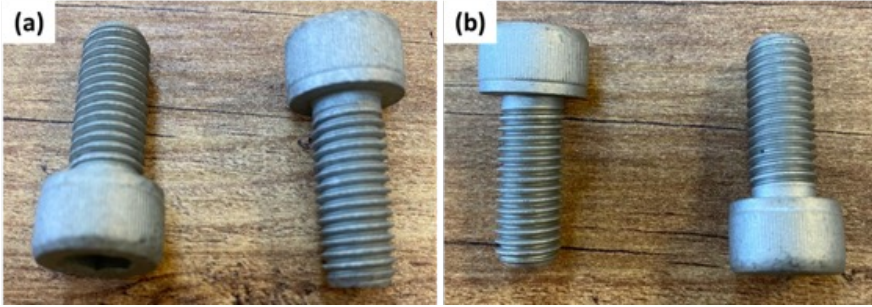
Şekil 3. Üretilmiş M10x25 DIN912 A2-70 paslanmaz test civataları.

getirmek ve paslanmaz çeliğin uzun süreli korozyon direncini sağlamak için pasivasyon yapılmaktadır. Pasivasyon tipik olarak paslanmaz çeliğin nitrik asit çözeltisine veya sitrik asit çözeltisine daldırılmasını içerir. Pasivasyon işlemi ayrıca paslanmaz çeliğin yüzeyinde bulunabilecek, kirlenici veya serbest demir iyonlarını da giderir. Pasivasyon işleminde öncelikle kir ve yağdan arındırılmıştır. Yüzeydeki pas tabakasının giderilmesi işlemi gerçekleştirilmiştir. Ardından yüzeydeki metalik tozların ve yağların tamamen giderilmesi sağlanmıştır. Nitrik asit çözeltisine alınan malzemeler burada pasivasyon işlemine tabi tutulmuştur. Son olarak durulama ve kurutma işlemleri ile pasivasyon işlemi tamamlanmıştır.

Geleneksel karbonlu çeliklerde yüzey kalitesinin iyileştirilmesi, sürtünme katsayılarının istenilen aralıkta ayarlanması ve korozyon direnci kazandırılması için yapılan kaplama işlemleri sektörde paslanmaz çeliklere de uygulanabilmektedir. Kaplama uygulanmadan önce, iyi bir yapışma sağlamak için civatanın yüzeyi hazırlanır ve çeşitli teknikler kullanılarak çinko lamelli kaplama uygulanabilir. Yaygın bir yöntem, kaplamanın civatanın tüm yüzeylerine eşit şekilde uygulanmasını sağlayan bir kaplama malzemesi banyosuna civataları batırmaktır. Alternatif olarak kaplama, özel donanım kullanılarak civatanın yüzeyine püskürtülebilir. Kaplama uygulandıktan sonra korozyona karşı dayanıklı ve etkili bir bariyer oluşturması için kütleme işlemi uygulanması gerekir. Bu çalışmada, sektörde sıklıkla kullanılan iki farklı ticari çinko lamelli kaplama ürünü ile civatalar kaplanarak korozyon direnci açısından pasivasyon işlemi ile karşılaştırmalı olarak incelenmiştir. Kaplamaların uygulama parametreleri Tablo 2'de gösterilmiştir. Her iki kaplama işlemi sonrasında kaplamalı örnekler Şekiller 6 (a) ve (b)'de görülmektedir.

Table 2. Test Prosedürü.

Kaplama	Program süresi	Kütleme Süresi	Kütleme Sıcaklığı
Kaplama 1	3 dakika	1 saat	180 °C
Kaplama 2	5 dakika	1.5 saat	250 °C



Şekil 6. (a) Kaplama 1 ve (b) Kaplama 2 uygulanmış test civataları.

Östenitik paslanmaz çelik civataların üretimleri tamamlandıktan sonra korozyon testleri gerçekleştirilmiştir. Korozyon testi olarak tuz püskürtme testi ISO 9227 standardına göre uygulanmıştır. Tuz püskürtme testi, pas ve korozyona karşı dirençlerini değerlendirmek için civatalar ve diğer metaller üzerinde gerçekleştirilen bir korozyon testidir. Her bir varyasyon için 5'er numune kullanılmıştır. Test, civataların kontrollü bir ortamda belirli bir süre boyunca tuz püskürtme sisine maruz bırakılmasıyla gerçekleştirilmiştir. Test tipik olarak kontrollü bir tuzlu su sisi oluşturabilen özel bir odada gerçekleştirilir. Oda, test koşullarını korumak için bir sıcaklık ve nem kontrol sistemi ile donatılmıştır. Civatalar test odasında üzerlerine önceden belirlenmiş bir oranda tuzlu su sisi püskürtülmüştür. Test sırasında, pas veya çukurlaşma gibi korozyon belirtileri olup olmadığını kontrol etmek için civatalar periyodik olarak incelenmiştir. Testler 24 saatlik periyotlarla gerçekleştirilmiştir. Testler tamamlandıktan sonra, temizlenip korozyon belirtileri açısından değerlendirilmiştir. Sonuçlar, civataların istenen korozyon direnci seviyesini karşılayıp karşılamadığını belirlemek için endüstri standartlarıyla karşılaştırılmıştır. Testlerde Liebisch 42016101 modeline sahip tuz püskürtme kabini kullanılmıştır (Şekil 7).

3. Bulgular ve Tartışma

Çalışmada, üretimleri tamamlanmış M10x25 DIN912 A2-70 paslanmaz çelik civata numunelerinin tuz püskürtme testleri gerçekleştirilmiştir. İlk aşamada doğrudan üretilmiş herhangi bir işlem yapılmamış civatalar tuz püskürtme testine tabii tutulmuştur. Numunelerde 48 saat sonunda civataların şaft, kafa ve soket bölgelerinde kırmızı oksitlenme tabakası (demir oksit) görülmüştür. Şekil 8'de teste ait test raporu ve test sonu civataların görselleri paylaşılmıştır. Malzemede herhangi bir kaplama olmadığı için beklendiği üzere beyaz oksidasyon görülmemiştir. İşlem görmemiş numunelerin tuz testi sonuçları paslanmaz çelikler için görece düşük korozyon direnci gösterdiği görülmektedir.

Pasivasyon işlemi uygulanmış olan civataların korozyon direncini belirlemek amacıyla tuz püskürtme testi gerçekle-



Şekil 5. Liebisch Model: 42016101 tuz püskürtme testi kabini.

tilmiştir. Teste ait rapor ve test sonu civata görselleri Şekil 9'da gösterilmiştir. Yapılan testlerde 1128 saat sonunda beyaz oksit tabakası görülmüştür. 1152 saat sonrasında özellikle kafa kısmında kırmızı oksit tabakası görülmüştür. Pasivasyon uygulanmamış civatalara yapılan testlere göre (48 saat) kırmızı oksit görülme süresi 24 kat artmıştır. Korozyon direnci konusunda pasivasyon işleminin kritik öneme sahip olduğu görülmüştür.

Şekil 10'da Kaplama 1 uygulanmış civataların tuz püskürtme testi sonuçları görülmektedir. Test sonucuna göre 192 saat sonunda beyaz oksit tabakası görülmüştür. Beyaz oksidasyon, kaplama malzemesinin içeriğinde yüksek oranda bulunan krom ve alüminyum elementlerinin oksitlenmesinden kaynaklanmaktadır. 504 saatlik test sürecinde sonunda kırmızı oksit görülmemiştir.

TEST RESULT & OBSERVATIONS	
White oxidation was observed at <i>Beyaz oksidin görüldüğü süre</i>	-
Red oxidation was observed at <i>Kırmızı oksidin görüldüğü süre</i>	48 hrs
Test duration <i>Test süresi</i>	48 hrs

Kırmızı oksit (Demir oksit)

Şekil 6. Pasivasyon işlemi yapılmamış civataların tuz püskürtme testi sonucu.

Şekil 11'de ise Kaplama 2 uygulanmış civataların tuz püskürtme testi sonuçları görülmektedir. Test sonucuna göre 288 saat sonunda beyaz oksidasyon görülmüştür. Test sonunda Kaplama 2 uygulanmış civatalarda da Kaplama 1 uygulanmış civatalara benzer olarak kırmızı oksit 594 saatlik test sonucunda görülmemiştir. Yapılan tüm testlerin ardından tüm malzemelerin tuz püskürtme test sonuçları Tablo 3'te birlikte verilmiştir. Pasivasyon işleminin yapılan kaplamalardan daha etkili bir korozyon direnci sağladığı açıkça görülmektedir. Kaplama 2'nin Kaplama 1'e göre 1.5 kat daha iyi bir korozyon direnci sağladığını da test sonuçları göstermiştir.

TEST RESULT & OBSERVATIONS	
White oxidation was observed at <i>Beyaz oksidin görüldüğü süre</i>	1128 hrs
Red oxidation was observed at <i>Kırmızı oksidin görüldüğü süre</i>	1152 hrs
Test duration <i>Test süresi</i>	1152 hrs



Şekil 7. Pasivasyon işlemi yapılmış civataların tuz püskürtme testi sonucu.

TEST RESULT & OBSERVATIONS	
White oxidation was observed at <i>Beyaz oksidin görüldüğü süre</i>	192 hrs
Red oxidation was observed at <i>Kırmızı oksidin görüldüğü süre</i>	-
Test duration <i>Test süresi</i>	504 hrs



Şekil 8. Kaplama 1 uygulanmış civataların tuz püskürtme testi sonucu.

TEST RESULT & OBSERVATIONS	
White oxidation was observed at <i>Beyaz oksidin görüldüğü süre</i>	288 hrs
Red oxidation was observed at <i>Kırmızı oksidin görüldüğü süre</i>	-
Test duration <i>Test süresi</i>	504 hrs



Şekil 9. Kaplama 2 uygulanmış yapılmış civataların tuz püskürtme testi sonucu.

Table 3. Tüm malzemelerin tuz püskürtme testi sonuçları.

Malzeme	Tuz Testi Sonucu Kırmızı Pas (saat)	Tuz Testi Sonucu Beyaz Pas (saat)
Pasivasyonsuz civata	48	-
Pasivasyonlu civata	1152	1128
Kaplama 1 uygulanmış civata	-	192
Kaplama 2 uygulanmış civata	-	288

4. Sonuçlar

Çalışma kapsamında günümüzde kullanımı git gide artmakta olan paslanmaz çelik civataların korozyon dirençleri tuz püskürtme testi ile incelenmiştir. Çalışmada paslanmaz çeliklere uygulanan pasivasyon işleminin korozyon direncine etkisinin incelenmesinin yanı sıra sektörde kullanılan çinko lamelli iki ticari kaplama uygulamasının da korozyon direncine etkisi incelenmiştir. Öncelikle pasivasyon işlemi yapılmadan üretimden direkt alınan numunelerine tuz püskürtme testi uygulanmıştır ve 48 saat sonunda beyaz pas oluşmadan doğrudan kırmızı pas oluştuğu görülmüştür. Bu durum malzemenin yüzeyindeki koruyucu krom oksit tabakası eksikliğini göstermiştir. Ardından pasivasyonlu test civataları tuz püskürtme testi uygulanmıştır. Pasivasyonlu civatalarda 1128 saat sonunda beyaz pas oluşmuş olup 1152 saat sonunda ise kırmızı pas oluşmuştur. Beyaz pas oluşumu pasivasyon işleminin doğru şekilde yapıldığını göstermektedir. Pasivasyonsuz çitallerle karşılaştırıldığında korozyon direncinde 24 kat artış olmuştur. Bu sonuç paslanmaz çelik civatalarda pasivasyon işleminin korozyon direnci açısından kritik rol oynadığını ortaya koymaktadır. Paslanmaz civatalara uygulanabilen ticari çinko lamelli kaplama türleri ayrıca korozyon dirençleri açısından kıyaslanmıştır. Sektörde sıklıkla kullanılan iki farklı kaplama çeşidi (Kaplama 1 ve Kaplama 2) test civatalarına uygulanmış ve tuz püskürtme testleri gerçekleştirilmiştir. Yapılan test sonucunda Kaplama 2 uygulanmış civatalar Kaplama 1

uygulanmışlara göre 1.5 kat yüksek korozyon direnci göstermiştir. Ancak pasivasyon işleminin sağladığı korozyon direnciyle kıyaslandığında kaplama işlemleri oldukça düşük kalmakta olduğu görülmüştür. Pasivasyonlu civatalar, Kaplama 2 uygulanmış civatalara göre yaklaşık 4 kat daha iyi korozyon direnci sergilemişlerdir. Kaplama işleminin maliyetleri ve uygulama zorlukları göz önünde bulundurulduğunda pasivasyon işlemiyle karşılaştırıldığında korozyon direnci özelinde anlamlı bir artış sağlamadığı ortaya çıkmıştır.

Teşekkür

Yazarlar çalışmanın yapılması ve sunulması konusunda sunduğu fırsat için Norm Holding'e teşekkür eder.

Kaynaklar

1. Davis, J.R., Stainless steels. 1994: ASM international.
2. Sheets, A.S.G.D., Atlas steels technical handbook of stainless steels. Stainless Steel, 2013. 630: p. 17-4PH.
3. ISO, E., 3506-1. Mechanical properties of corrosion-resistant stainless steel fasteners-Part 1: Bolts, screws and studs (ISO 3506, 1997. 1.
4. Maller, R.R., Passivation of stainless steel. Trends in food science & technology, 1998. 9(1): p. 28-32.
5. ASTM, A., 967-05. Standard specification for chemical passivation treatments for stainless steel parts. West Conshohocken: ASTM, 2005.
6. ISO, E.I.E., 9227 (2017). Corrosion tests in artificial atmospheres-Salt spray tests. Search in, 2020.
7. Tsutsumi, Y., A. Nishikata, and T. Tsuru, Pitting corrosion mechanism of Type 304 stainless steel under a droplet of chloride solutions. Corrosion science, 2007. 49(3): p. 1394-1407.
8. Wang, J., et al., Fatigue behaviour of stainless steel bolts in tension and shear under constant-amplitude loading. International Journal of Fatigue, 2020. 133: p. 105401.
9. Byun, J.B., et al., Automatic multi-stage cold forging of an SUS304 ball-stud with a hexagonal hole at one end. Materials, 2020. 13(22): p. 5300.
10. Tianxiong, Z., et al., Experimental study on mechanical properties and tightening method of stainless steel high-strength bolts. Engineering Structures, 2023. 290: p. 116176.

MAXIMIZING DIE LIFE IN COLD FORGING DIES FOR FASTENER PRODUCTION: PARAMETER DETERMINATION AND OPTIMIZATION

Sezgin YURTDAS
Levent AYDIN
Ömer EYERCIOĞLU



8th International New York Conference On Evolving Trends in Interdisciplinary Research & Practices

MAXIMIZING DIE LIFE IN COLD FORGING DIES FOR FASTENER PRODUCTION: PARAMETER DETERMINATION AND OPTIMIZATION

Sezgin Yurtdas^{1*}, Levent Aydin², Omer Eyercioglu³

¹The Graduate School of Natural and Applied Sciences, İzmir Katip Çelebi University, İzmir, Turkey.

²Department of Mechanical Engineering, İzmir Katip Çelebi University, İzmir, Turkey.

³Department of Mechanical Engineering, Gaziantep University, Gaziantep, Turkey.

*sezgin.yurtdas@normfasteners.com, ORCID 0000-0002-4120-8882, +1-5177759295

²levent.aydin@ikcu.edu.tr

³eyercioglu@gantep.edu.tr

Abstract

In this study, the aim was to develop a numerical model to estimate the realistic die life under production line conditions of axially symmetric cold forging dies used in fastener production and maximize the die life. The study determined that Morrow's equation which is commonly used in determining die life in the cold forming industry, causes high scattering in production line trials. Hence, the study revised the fatigue strength coefficient (σ') and fatigue strength exponent (b) of the relevant equation using production line and numerical simulation data from four different cold forging dies. The revised model has been found to be compatible with the production line data. Using a D-Optimal experimental design in a selected axisymmetric head forging die, 3D modeling and numerical studies were carried out for various levels of four different cold forging die manufacturing parameters to determine die life values. In the study, a D-Optimal experiment design was conducted using Design Expert. Design studies were performed in Catia and material flow and tool life analyses were carried out using Simufact.forming software. The data obtained from these numerical studies were utilized in modeling studies conducted in Mathematica software. The study evaluated the models created from ten different data groups based on $R_{z\text{training}}$ and $R_{z\text{testing}}$. Optimization studies were also discussed, using Random Search, Differential Evolution, Nelder Mead and Simulated Annealing methods. The results of the five different scenarios in four different algorithms were obtained for second-order trigonometric multiple nonlinear (SOTN) and second-order logarithmic multiple nonlinear (SOLN) models. Considering the manufacturing precision of cold forging dies in the optimization studies, the maximum die life for the SOLN model was determined as 497,299 in the study.

Keywords: cold forging, fastener, modeling, optimization

THE INVESTIGATION OF MECHANICAL PROPERTIES AND PERFORMANCE OF ADDITIVELY MANUFACTURED STAINLESS STEEL BOLTS

Burak HIZLI
 Sarper DOĞAN
 M. Burak TOPARLI
 Umut İNCE
 Paul BOREHAM
 Kyriakos KOUROUSIS



International Conference on Materials Science and Manufacturing - ICMSM 2023

THE INVESTIGATION OF MECHANICAL PROPERTIES AND PERFORMANCE OF ADDITIVELY MANUFACTURED STAINLESS STEEL BOLTS

Burak Hizli¹, Sarper Dogan², M. Burak Toparli³, Umut Ince⁴, Paul Boreham⁵, Kyriakos Kourousis⁶

¹R&D Center, Norm Izmir Civata San. Tic. A.Ş., burak.hizli@normfasteners.com

²R&D Center, Norm Izmir Civata San. Tic. A.Ş., sarper.dogan@normfasteners.com

³R&D Center, Norm Izmir Civata San. Tic. A.Ş., burak.toparli@normfasteners.com

⁴R&D Center, Norm Izmir Civata San. Tic. A.Ş., umut.ince@normfasteners.com

⁵School of Engineering, University of Limerick, paul.boreham@ul.ie

⁶School of Engineering, University of Limerick, kyriakos.kourousis@ul.ie

Abstract

In recent years, additive manufacturing of metallic materials has become one of the most interested manufacturing method in terms of beneficial capabilities over free-form modelling, rapid prototyping, and less material waste. Therefore, it enables to create complicated components for various applications in different industries. For the fastener industry, cold forming operation is an efficient and proven method for mass production, on the contrary, additive manufacturing can be implemented in production of stainless steel fasteners, which have certain restrictions for cold forming considering high forging load requirements and decreased performance of forming dies. In the scope of this study, M5 stainless steel bolts produced from 316L powder by additive manufacturing were compared to AN3-4A steel bolts and M5 8.8 grade steel bolts produced by 23MnB4 carbon steel based on the performance during tightening process. Hence, breaking torque tests were carried out. According to the results, additively manufactured bolts reached the highest breaking torque values in 60° orientation compared to other orientations. Additionally, those bolts exhibited lower breaking torque performance than that of both AN3-4A steel bolts and 8.8 grade steel bolts. Thereafter, fracture surfaces of tested bolts were examined using SEM in order to understand the failure at lower breaking torques. It was seen that fracture initiated in the lack-of-fusion zones and partially melted zones due to higher stress concentration as a result of torsion.

Keywords: Metal additive manufacturing, stainless steel, steel, bolt, breaking torque

AN INVESTIGATION OF THE FATIGUE LIFE OF WC- 26 WT.% CO MATERIAL USED IN COLD FORGING DIES

Burak HIZLI
Kubra ÖZTÜRK
M. Burak TOPARLI
Umut İNCE



International Conference on Materials Science and Manufacturing - ICMSM 2023

AN INVESTIGATION OF THE FATIGUE LIFE OF WC- 26 WT.% CO MATERIAL USED IN COLD FORGING DIES

Burak Hizli¹, Kubra Ozturk², M. Burak Toparli³, Umut Ince⁴

¹R&D Center, Norm İzmir Civata San. ve Tic. A.Ş., burak.hizli@normfasteners.com

²R&D Center, Norm İzmir Civata San. ve Tic. A.Ş., kubra.ozturk@normfasteners.com

³R&D Center, Norm İzmir Civata San. ve Tic. A.Ş., burak.toparli@normfasteners.com

⁴R&D Center, Norm İzmir Civata San. ve Tic. A.Ş., umut.ince@normfasteners.com

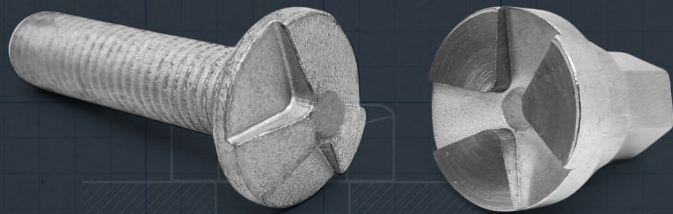
Abstract

The cold forming of fasteners requires high forging forces, which cause significant stresses in the dies. WC-Co materials are preferred for use in die materials in the production of fasteners through cold forging, due to their high strength, wear resistance, high hardness, and low elastic deformation characteristics. Precise estimation of die life is critical for enhancing production efficiency and reducing die-related expenditures especially in the cold forging processes. The aim of this study was to reveal the fatigue behavior of WC-Co materials with a Co content of 26%, which are commonly used in forging dies. Experimental investigations were to determine and compare the fatigue performance at three different stress amplitudes using three-point bending fatigue testing of WC-%26 wt Co. To investigate the fatigue behavior under a wide range of loading conditions, three stress amplitudes of 750, 800, and 850 MPa corresponding to 25%, 27%, and 28.3% of compressive strength of WC-%26 wt Co. were selected for fatigue testing. Maximum and minimum stress values were calculated for stress ratio of R0.1 and R0.2. Loading frequency in fatigue testing was set to 72.45 Hz. The fatigue performance of each set was determined from the mean of at least three test results. After completing the experiments Goodman-Haigh diagrams were obtained from the experimental results.

Keywords: WC-Co, Co ratio, Fatigue life, Cold forming

A CASE STUDY OF THE EFFECT OF ELEMENT TYPE ON THE NUMERICAL SIMULATION RESULTS OF FASTENER COLD FORGING PRODUCTION

Mert ÖZDOĞAN
Hatice SANDALLI YILDIZ



12. Uluslararası Mühendislik Mimarlık ve Tasarım Kongresi, 12th International Congress on Engineering, Architecture and Design. 23-25 Aralık İstanbul

A CASE STUDY OF THE EFFECT OF ELEMENT TYPE ON THE NUMERICAL SIMULATION RESULTS OF FASTENER COLD FORGING PRODUCTION

Mert ÖZDOĞAN¹, Hatice SANDALLI YILDIZ¹

¹Norm Fasteners, İzmir/TURKEY

Abstract

Finite element solution of any mathematical model requires discrete finite elements (FE) or mesh, and accuracy of finite element analysis (FEA) significantly depends on it. Increasing the element count, in most cases, improves the accuracy of FEA, but it yields to a higher computational power. Altering the order of shape functions or elements degrees of freedom (DOF) is another approach to achieve decent accuracy with less element count, but, it is crucial to choose right element type in order to get real-like physical results. In this study, FE with various DOF are examined for deformation process of hexagon weld nut. FE analysis are conducted on Simufact. Forming for mesh types with increasing DOF; tetrahedral(134), tetrahedral(157) and tetrahedral(247), in order to investigate the effect of element type on cold forging simulation. Results are compared with hexahedral mesh, which is recommended element type by Simufact, for effective plastic strain, contact pressure, geometrical accuracy and required forging power. It is found that for equal element count, geometry is almost same for all tetrahedral types and they are similar to hexahedral mesh. Tetrahedral(134) results found to be disproportional in the sense of plastic strain and contact pressure, compared to reference mesh and should be avoided for current case. Tetrahedral(157) and tetrahedral(247) yield to similar results but the latter can compute quadruply faster and its results are more similar to hexahedral mesh. Correlation between DOF and FEM accuracy is observed. It is suggested that for such plastic deformation problem, elements with high DOF is found to be more convenient.

Keywords: Finite Element Analysis, Degree of Freedom, Cold Forging Simulation, Mesh Type

INVESTIGATION OF THREADING PERFORMANCE OF SELF-THREADING NUTS ON MACHINED AND CASTED ALUMINUM PARTS

*Burak Berk ARINCI
Hatice SANDALLI YILDIZ
Umut İNCE
Muhammed Burak TOPARLI
Niyazi Emrah KILINÇDEMİR
Sarper DOĞAN*



12. Uluslararası Mühendislik Mimarlık ve Tasarım Kongresi, 12th International Congress on Engineering, Architecture and Design. 23-25 Aralık İstanbul

INVESTIGATION OF THREADING PERFORMANCE OF SELF-THREADING NUTS ON MACHINED AND CASTED ALUMINUM PARTS

Burak Berk ARINCI¹, Hatice SANDALLI YILDIZ¹, Umut İNCE¹, Muhammed Burak TOPARLI¹, Niyazi Emrah KILINÇDEMİR², Sarper DOĞAN¹

¹Norm Fasteners, İzmir/ TURKEY

²Norm Fasteners Co., Michigan/ USA

Abstract

Due to changing industry needs and increasing costs, reduced process steps and assembly time are essential. Self-threading nuts are the products that develops for this purpose. A standard nut is threaded into a round hole, then assembled with a counterpart threaded with a tapping, and assembled at the relevant location. The threading processes of the two parts are carried out separately, causing input costs and loss of time. Self-threading nuts are used in assemblies by creating thread on counterpart with the thread structure they have. Thanks to this feature, they eliminate the need for tapping threads separately, making the installation process faster and more straightforward. In this study, the threading performance of four lobular, patent pending, self-threading nuts were investigated. The nuts were manufactured with cold forging and threads were formed with tapping. Heat treatment was applied to obtain required mechanical properties. Counterpart to be threaded was selected as aluminum with a hardness of 110 HV. Two sets of counterparts were manufactured. The first group was manufactured with machining, while the second group was manufactured with casting. These two groups were further divided into two in terms of taper angle. Based on the experimental results, it was revealed the quality of formed threads was directly correlated with porosity level of the casted aluminum counterparts. It was seen that machined counterparts were able to withstand higher torque than casted parts. Furthermore, in terms of thread quality and threading performance, the diameter of the counterpart was found to be another critical factor.

Keywords: Cold Forging, Thread Forming, Self-threading Nut



NORM
FASTENERS



www.normfasteners.com